

**Studies on Prediction Systems for Revealing Biological Functions of Drug Candidates**

**January 2019**

**Yasunori FUKUDA**

**Studies on Prediction Systems for Revealing Biological Functions of Drug Candidates**

**A Dissertation Submitted to  
the Graduate School of Life and Environmental Sciences,  
the University of Tsukuba  
in Partial Fulfillment of the Requirements  
for the Degree of Doctor of Philosophy in Biological Science  
(Doctoral Program in Biological Sciences)**

**Yasunori FUKUDA**

## **Table of contents**

<b>General Abstract</b> .....	4
<b>Abbreviations</b> .....	7
<b>General Introduction</b> .....	9
<b>Chapter I</b> .....	15
<b>Abstract</b> .....	16
<b>Introduction</b> .....	17
<b>Results</b> .....	19
<b>Discussion</b> .....	24
<b>Conclusion</b> .....	26
<b>Methods</b> .....	27
<b>Tables and Figures</b> .....	31
<b>Chapter II</b> .....	55
<b>Abstract</b> .....	56
<b>Introduction</b> .....	57
<b>Materials and methods</b> .....	59
<b>Results</b> .....	62
<b>Discussion</b> .....	65
<b>Tables and Figures</b> .....	68
<b>General Conclusion</b> .....	86
<b>Acknowledgement</b> .....	88
<b>References</b> .....	90

## General Abstract

Various types of biological reactions are critical for maintaining the functions of cells, the fundamental units of our body. Biological molecules such as DNA and proteins play an important role in these reactions. Furthermore, biomolecular dysfunction caused by cellular stresses, such as DNA mutations, lead to the overactivation or suppression of molecular functions, resulting in the disruption of cellular homeostasis. This disruption gives rise to diseased states, and drugs are utilized to ameliorate these molecular dysfunctions. Recently, genetic technologies such as siRNA and CRISPR have been used widely to clarify the functions of molecules and pathogenic mechanisms. Additionally, chemical compounds that specifically regulate the functions of target proteins are powerful tools to understand biological phenomena.

In drug discovery research, drug candidates are developed to effectively ameliorate biological dysfunctions occurring in diseased states. However, recent post-marketing surveillances and clinical studies have revealed that some marketed drugs and candidates are withdrawn due to unexpected adverse effects through the induction of detrimental cellular phenotypes. These detrimental phenotypes are considered to be caused by unintentional/off-target interactions of the drugs/candidates. In addition, it is still difficult to predict and detect these adverse phenotypes in the non-clinical research stages due to the lack of highly physiologically relevant *in vitro* models. For the development of safer drugs, it is critically important to accurately detect adverse drug effects in the early phase of drug discovery research. From this point of view, I considered that there were two critical issues to be solved in *in vitro* toxicology. The first one is the difficulty of identifying off-target molecules, and the second is the lack of *in vitro* models recapitulating drug toxic responses in human bodies.

In my study, to address the first issue, I developed a pathway profiling system to identify drug off-targets with a simple and efficient method. In one example, 2-amino-4-(3,4-

(methylenedioxy)benzylamino)-6-(3-methoxyphenyl)pyrimidine, a Wnt agonist, was identified as a senescence inducer through phenotypic screening. To identify its target proteins, I compared a series of cellular assay results with those of a pathway profiling database comprising the activities of compounds as determined using simple assays of cellular reporter genes and cellular proliferation. In this database, compounds were classified based on the statistical analysis of their activities, which corresponded to the mechanism of action of representative compounds. In addition, the mechanisms of action of the compounds of interest could be predicted using the database. Based on my database analysis, the compound was predicted to be a tubulin disruptor, and this prediction was subsequently confirmed from its inhibition of tubulin polymerization.

To address the second issue, I developed a highly physiologically relevant assay system for the specific detection of drug-induced renal toxicities. As drug candidates are sometimes withdrawn owing to renal toxicity, the accurate prediction of drug-induced renal toxicity is necessary for the development of safer drugs. Cellular assay systems that recapitulate physiologically relevant microenvironments have been proposed for obtaining a good estimation of drug responses in the human body. However, establishment of such assay systems for accurate prediction of renal toxicity is challenging due to the lack of readily available *in vitro* assay systems. In my study, I investigated the cellular response to fluid shear stress, a characteristic of physiological environments in the kidney proximal tubules, using microfluidic devices. The global gene expression profiles of human primary proximal tubule cells under the fluidic conditions revealed the upregulation of MATE2-K and activation of Nrf2 signaling in response to the fluid shear stress. Moreover, a bioinformatic analysis and cellular biological assay revealed that the expression of MATE2-K is regulated by Nrf2 signaling. These results strongly suggest that fluid shear stress, a major physical stress in tissues, is involved in the expression and functional maintenance of tissue-specific drug transporters in the proximal tubule, where the cells are exposed to continuous shear stress by primary urine.

My first study emphasizes that the pathway profiling database is a simple and potent tool for revealing off-targets, that induce adverse drug effects of drugs and drug candidates. My second study demonstrates that the microfluidic culture of human proximal tubules could be a useful system to accurately predict drug renal toxicities under physiologically relevant conditions. I conclude that both of my developed platforms provide researchers tools to detect cellular toxicities and off-targets. This consequently contributes to the selection of appropriate drug candidates to develop safer and more effective drugs. Moreover, these platforms can be applied not only to detect drug responses, but also to reveal novel gene functions, in combination with current molecular biological methods such as gene-editing technologies.

## Abbreviations

AMBMP	2-amino-4-(3,4-(methylenedioxy)benzylamino)-6-(3-methoxyphenyl)pyrimidine
BARD	bardoxolone methyl
CRISPR	clustered regularly interspaced short palindromic repeats
dPPA	12-deoxyphorbol 13-phenylacetate 20-acetate
ECM	extracellular matrix
FDA	The Food and Drug Administration
FSS	fluid shear stress
HCS	high-content screening
hERG	human Ether-a-go-go Related Gene (KCNH2)
HNF	hepatocyte nuclear factor
HTS	high-throughput screening
iPS cell	induced pluripotent stem cell
MOA	mechanism of action
NECA	N-ethylcarboxamidoadenosine
OAT	organic anion-transporting protein
PDD	phenotypic drug discovery
PDE	phosphodiesterase
PMA	phorbol 12-myristate 13-acetate

PTEC	proximal tubule epithelial cell
ROS	reactive oxygen species
SLC	solute carrier proteins
WGCNA	weighted gene co-expression network analysis

## **General Introduction**

Numerous biological reactions maintain the functions of cells, which are the fundamental units of our body. Biological molecules such as DNA and proteins play an important role in these reactions. Although the complete human genome sequence has been revealed, functions of several genes remain to be clarified. To identify their functions in cells, genetic techniques such as siRNA and CRISPR have been utilized widely [1]. Additionally, chemical probes that modulate the function of target proteins are powerful tools for understanding biological phenomena [2].

Biomolecular dysfunctions caused by cellular stresses, such as DNA mutations, lead to the overactivation or suppression of molecular functions. This results in the disruption of cellular homeostasis. This disruption gives rise to diseased states, and drugs are generally utilized to ameliorate these molecular dysfunctions. For instance, a genetic mutation of NLRP3, which is an inflammasome component and participates in eliminating pathogens, causes the overactivation of inflammatory reactions such as IL1 $\beta$  production and secretion, causing autoinflammatory diseases [3]. To treat these diseases, NLRP3 inhibitors and anti-IL1 $\beta$  antibodies have been developed as anti-autoinflammatory drugs to restore inflammasome homeostasis [4]. In basic research, these drugs, especially small molecule compounds, are utilized as chemical probes to understand inflammasome signaling [5].

In drug discovery research, drug candidates are developed to potentially normalize the functions of target molecules whose dysfunctions causes the diseased states. In general, these small molecules regulate biological functions by acting as inhibitors or activators of target molecules. However, post-marketing surveillance and clinical studies have revealed that some drugs and candidates exert not only primary pharmacological effects, but also some adverse effects through the induction of detrimental phenotypes such as apoptosis [6]. These detrimental phenotypes are considered to be caused by interaction with off-target molecules [7]. So far, small molecules have been believed to regulate only the functions of their target molecule, but recently it has been revealed that drug candidates likely have multiple targets in our bodies [8].

The off-target molecules that interact with drug candidates are not readily identified under regular research strategies. Thus, it is particularly difficult to detect detrimental phenotypes using typical animal and cell models, as they do not completely recapitulate the conditions in human bodies [9-13]. Therefore, translational research has recently attracted attention with increased focus on connecting basic research and clinical events [14, 15]. In particular, adverse drug reactions caused by unknown off-target molecules have been primary cause of failures in drug discovery research [16]. An analysis of the reasons for failure of drug candidates has revealed that a large number of candidates are withdrawn owing to safety issues [17]. This analysis showed that non-clinical toxicology and clinical safety were the main reasons for termination, portions of which were over 50% in total [17]. In addition, some drugs were withdrawn after launch due to severe side effects. For example, the antihistamine terfenadine, a predecessor of fexofenadine, was withdrawn because it caused arrhythmias, which have been attributed to the off-target inhibition of the hERG channel [18]. Similarly, haloperidol, presently treated as a typical antipsychotic medication, is an inverse agonist of the dopamine D2 receptor. The compound is reported to bind other dopamine receptors, 5HT receptors, and adrenergic receptors, leading to adverse effects such as akathisia and hypotension [19]. Furthermore, haloperidol was found to inhibit mitochondrial complex I in an off-target interaction, generating adverse effects involving the extra-pyramidal tract [20].

Although numerous cutting-edge technologies, such as induced pluripotent stem (iPS) cells and next-generation sequencing, have been employed in drug discovery research, it is still difficult to predict the off-target molecules responsible for specific adverse effects in the body. Recently, other than experimental efforts, some researchers have also attempted to utilize biological assay data of a large number of compounds to predict adverse effects. Lounkine et al. [21] employed the Similarity Ensemble Approach (SEA), which calculates whether a molecule will act on a target based on the chemical structure it shares a known ligand. This analysis predicted the activity of 656 marketed drugs

on 73 unintended off-target molecules. However, only half of the predictions were found to be accurate [21]. At present, deep learning, a representative artificial intelligence (AI) technology, has been introduced to predict drug toxicities using databases of chemicals and drugs analyzed by various bioassays, but the toxicity prediction rate needs further improvements [22].

To effectively develop safer drugs, it is essential to accurately detect adverse drug effects and reveal their molecular mechanisms in the early phase of drug discovery research. From this point of view, I considered that there are two critical issues to be addressed in *in vitro* toxicology. The first is the difficulty of identifying unknown off-target molecules, because there are many kinds of off-target candidates that could cause adverse effects in our bodies. To date, the target identification methods developed are all based on chemical proteomics. These methods have revealed many unique target proteins associated with bioactive compounds. For example, by using this technology, thalidomide, a drug for morning sickness during early pregnancy, was proven to bind to cereblon, an E3 ligase, thereby clarifying the molecular mechanism of its teratogenic effects [23]. However, because this method is based on an affinity pull-down assay, it requires further chemical synthesis to add chemical tags to compounds of interest without decreasing their biological activities [24]. For tagless determination of the target molecules of compounds, Petrone et al. developed the chemical biological descriptor “high-throughput screening finger print (HTS-FP)”, which employs accumulated HTS data [25]. From the perspective of the pharmaceutical industry, target identification methods with a simple system are highly desirable.

The second issue is the difficulty of recapitulating toxic drug responses in human bodies using *in vitro* cellular assay systems. In toxicology, animal models and *in vitro* models comprising human cell lines are commonly employed. However, these typical systems do not accurately mimic tissue functions. This is due to species-specific differences in gene sequences and expression patterns in animal models and the lack of functional proteins in cellular models [9, 13]. Regarding studies on

drug-induced nephrotoxicity, the expression of mRNA for kidney-specific drug transporters in HK2 cells, a widely used human proximal tubule cell line, was reported to be much lower than that in kidney cortex tissue samples [26]. With the advancement of stem cell technologies such as iPS cells and ES cells have, researchers can easily access various types of human cells that are not technically fresh human primary tissues such as neuronal cells [27, 28]. These stem cell-derived cells are confirmed to express some tissue-specific genes, but they still have some limitations regarding the diversity of iPS cell characteristics, iPS cell differentiation efficiency, and their cellular functions [28-30]. Currently, these cells are differentiated using only humoral factors, including various kinds of growth factors. Considering the tissue environments, each cell should be cultured in conditions facilitating interactions with other types of cells and exposure to physical stresses such as shear stress induced by the bloodstream. These stresses are now believed to be important factor for the recapitulation and maintenance of the physiological functionality of human organs and for committing the stem cells to a specific lineage [31-33]. Therefore, other than humoral factors, the physical environmental factors in tissues must be taken into account when establishing microphysiological organ models.

Organ-on-chips, one of the *in vitro* organ models, are microengineered biomimetic systems that represent key functional units of human organs and recapitulate cell-cell interactions and mechanical microenvironments. These systems are used as specialized *in vitro* models to investigate pharmacological and toxicological modulation of complex biological processes. For instance, to predict hepatotoxicity, one of main reasons for clinical trial failures, many research groups and biotech companies have made efforts to develop *ex vivo* hepatic culture systems, i.e., liver-on-a-chip, with nutrient and oxygen gradients and shear stress, which are important for maintaining hepatocyte functions [34, 35].

In my study, to address the above two issues related to the high attrition rates in drug discovery, I developed two systems to evaluate drug adverse effects in the early phase of drug

discovery. In chapter I, I describe the development of the pathway profiling system, which identifies off-target molecules inducing cell toxicities, with a simple target identification approach involving tag-free compounds. Also, I reveal an off-target molecule of AMBMP, a widely used Wnt signaling activator, using this system. In chapter II, I describe the development of a highly physiologically relevant cellular assay system to detect adverse drug effects in kidney proximal tubules. Using the assay system, I reveal that the expression of MATE2-K is regulated by Nrf2 signal induced by shear stress.

## **Chapter I**

**Tubulin is a molecular target of the Wnt-activating chemical probe**

## Abstract

In drug discovery research, cell-based phenotypic screening is an essential method for obtaining potential drug candidates. Revealing the mechanism of action is a key step on the path to drug discovery. However, elucidating the target molecules of hit compounds from phenotypic screening campaigns remains a difficult and troublesome process. Simple and efficient methods for identifying the target molecules are essential.

2-Amino-4-(3,4-(methylenedioxy)benzylamino)-6-(3-methoxyphenyl)pyrimidine (AMBMP) was identified as a senescence inducer from a phenotypic screening campaign. The compound is widely used as a Wnt agonist, although its target molecules remain to be clarified. To identify its target proteins, I compared a series of cellular assay results for the compound with my pathway profiling database. The database comprises the activities of compounds from simple assays of cellular reporter genes and cellular proliferations. In this database, compounds were classified on the basis of statistical analysis of their activities, which corresponded to a mechanism of action by the representative compounds. In addition, the mechanisms of action of the compounds of interest could be predicted using the database. Based on my database analysis, the compound was anticipated to be a tubulin disruptor, which was subsequently confirmed by its inhibitory activity of tubulin polymerization.

These results demonstrate that tubulin is identified for the first time as a target molecule of the Wnt-activating small molecule and that this might have misled the conclusions of some previous studies. Moreover, the present study also emphasizes that my pathway profiling database is a simple and potent tool for revealing the mechanisms of action of hit compounds obtained from phenotypic screenings and off targets of chemical probes.

## **Introduction**

Drug candidate selection through small-molecule screening is a rational and widespread method in the current drug discovery cascade. Initially, drug discovery research involved cell-based phenotypic screening as a core approach to obtaining drug candidates [36]. However, since the completion of the Human Genome Project in 2003 and the finding that sequences include numerous potential target proteins for drug discovery, target-based drug screening has been pursued actively [37, 38]. In addition, target-based drug screening procedures were initially accelerated to increase the research and development productivity of drug discovery in pharmaceutical companies. However, the number of FDA-approved drugs screened from the target-based approach was much less than expected because a large number of drug candidates failed during drug development owing to safety issues and a lack of efficacy [16]. In contrast, recent analysis of all first-in-class new molecular entities showed that phenotypic screening approaches accounted for 37% in comparison with 23% from target-based approaches [36]. Accordingly, classical cellular phenotypic screenings, also called phenotypic drug discovery (PDD), are being reevaluated as complementary and efficient strategies for probing drug candidates.

Chemical probes are powerful tools for target validation of hit compounds from PDD. However, some well-known chemical probes have been used incorrectly and have resulted in misleading biological conclusions [39]. Therefore, target identification of these compounds is essential for PDD. To date, target identification methods that use chemical proteomics or activity-based proteomics have been developed, and they have uncovered many unique target proteins associated with bioactive compounds [24, 40]. Although this is certainly a useful method, it requires mass spectrometry instrumentation and further chemical syntheses to add tags to compounds of interest without deteriorating their activities. To determine the target molecules of compounds without affinity tags, Petrone et al. developed the chemical biological descriptor “high-throughput screening

finger-print (HTS-FP)” that employs accumulated HTS data [25]. On the other hand, Frederick et al. developed a screening platform that consists of a series of reporter gene assays to disclose the mechanism of actions (MOAs) of compounds and by conducting assays in a quantitative HTS format [41, 42]. To develop a much simpler target identification approach with tag-free compounds, I exploited a pathway profiling database using only tens of cellular assays representing cellular signaling cascades through evaluation of compounds at a single concentration.

Oncology has become one of the largest therapeutic areas in the pharmaceutical industry. Various kinds of molecular targets and cellular signals have been reported to inhibit cancer growth. Among them, cellular senescence is considered to be the most important cellular phenotype for permanently arresting the cell cycle [43]. To date, reports have shown that genetic mutations and cellular stressors such as oxidative stress enhance cellular senescence and that some small molecules induce cellular senescence [44, 45]. In particular, compounds that induce cellular senescence are expected to be potent drugs for suppressing cancer growth [46]. Here I conducted a phenotypic screening campaign based on high-content cellular imaging to probe small molecules that induce cellular senescence.

## Results

### Pathway profiling database classifies compounds according to their MOA

The pathway profiling database mainly comprises reporter gene assays using firefly luciferase that cover 13 different signaling pathways and cellular proliferation assays with 7 commercially available cell lines (Table 1). These types of cellular assays are widely used in cell biology research and are highly accessible because of their simple procedures and low cost. In addition, these assays are very robust and demonstrate high throughput, which enabled us to detect subtle signal changes in an HTS-compatible format. The assays were functionally validated using the dose-dependent response of a native ligand or known inhibitors/activators.

Through the development of this database, I evaluated 1,910 compounds from 3 commercial compound libraries that contained compounds with well-characterized MOAs and common experimentally used reference compounds. I evaluated these libraries at a single concentration of 3  $\mu\text{g/mL}$  for the Natural Product Library and at 3  $\mu\text{M}$  for the other libraries. After obtaining all data, the database was analyzed using hierarchical clustering of the activities using Ward's method in TIBCO Spotfire software (Figure 1A). As a result of the hierarchical clustering analysis, compounds that had similar activities in most assays were classified into the same cluster, enabling me to visually determine that they have similar molecular targets and signaling pathways.

Forskolin (Figure 2), an adenylyl cyclase activator [47], was included in each library, and all were grouped into one cluster (Figure 1B). In the cluster, N-ethylcarboxamidoadenosine (NECA) (Figure 2), an adenosine receptor agonist [48], was also included. This cluster was shown to gather compounds stimulating cAMP production via adenylyl cyclase activation. This result indicates that the pathway profiling database classifies compounds according to their MOA. Similarly, phorbol 12-myristate 13-acetate (PMA) [49] and its structural analogs phorbol 12,13-dibutyrate [50], 13-O-acetylphorbol [51], and 12-deoxyphorbol 13-phenylacetate 20-acetate (dPPA) [52] (Figure 2) were

classified into the same cluster (Figure 1C). In other words, the structural analogs that had the same effect on cellular signaling were categorized into one cluster, as expected.

Following these analyses, I investigated structurally diverse compounds that affect the same target proteins. I focused on the phosphodiesterase (PDE) inhibitors [53-56] (Figure 2) contained in my database. To quantitatively compare differences in the structures and activities of each compound in my database, I employed Tanimoto structural similarity calculated by Daylight's fingerprints and Pearson's correlation coefficients (activity versus activity), respectively. The Tanimoto similarities ranged from 0.16 to 0.65, strongly indicating the broad structural diversity between the compounds in my database (Figure 1D). In contrast, Pearson's correlation coefficients (activity versus activity) in my database ranged from 0.64 to 0.83 (Figure 1D), showing their high bioactive similarities, despite their low structural similarities. These results indicate that my pathway profiling database based on the biological activities of compounds led to classifications corresponding to not only their structural similarities but also their MOAs.

### **Wnt-activating small molecule is identified as a cellular senescence inducer**

Triple-negative breast cancer has been a focus among the various cancer classes because of its lack of response to hormonal therapies, and new drugs with distinct MOAs are absolutely required to cure breast cancer patients [57]. Therefore, I employed MDA-MB-231 cells with triple-negative features to obtain cellular senescence inducers as anticancer agents [58]. In this strategy, I performed phenotypic screening on the basis of high-content cellular imaging, which is a very useful method to analyze altered cellular morphology. The cellular senescence morphology was reported to lead to a topologically enlarged appearance [43]. Sodium butyrate is a well-known senescence inducer [59], and I confirmed that it provoked the reported senescence phenotype in MDA-MB-231 cells and expanded cell shapes (Figure 3A). In my study, this cellular morphology was defined as an indicator

of cellular senescence.

For high-content screening (HCS) of senescence inducers, I developed a cell-based assay to analyze cellular phenotypic changes in MDA-MB-231 cells. To determine the activities of compounds in this HCS, the cellular area, which plays a key role in the selection of senescence inducers, was calculated using a custom-made image analysis algorithm. I screened 1,408 compounds in Tocriscreen (TOCRIS Bioscience) and StemSelect Small Molecule Regulators (Merck Millipore) at concentrations of 3  $\mu$ M and obtained 20 compounds that induced a  $\geq 2$ -fold enlargement of the cytosolic area (Figure 3B). Of these 20 compounds identified as senescence inducers (Figure 3C), molecular targets of 19 compounds have been clarified in past studies, but that of 2-amino-4-(3,4-(methylenedioxy)benzylamino)-6-(3-methoxyphenyl)pyrimidine (AMBMP) (Figure 2) has not been revealed yet. Thus, I focused on AMBMP to elucidate its molecular target, which is described further in this report.

It is generally considered that Wnt signaling pathways play important roles during embryonic development [60]. AMBMP was first identified as a Wnt signal agonist through Wnt signal activator screening using a common reporter gene assay [61]. To date, the first report of AMBMP has been cited in 68 papers, and the compound itself and its 10 applications have been patented (SciFinder®). However, its binding proteins have not yet been identified. I initially measured the activity of AMBMP using a Wnt reporter gene assay, as reported previously by Liu et al. [61]. Unexpectedly, using the Wnt reporter assay, I detected a much lower efficacy of AMBMP than that of a widely known Wnt signal activator glycogen synthase kinase 3 $\beta$  (GSK3  $\beta$ ) inhibitor (SB216763) [62] (Figures 2 and 3D). In contrast, GSK3  $\beta$  inhibitors were not observed to induce the senescence morphology (Figure 3E, Figure 4). These results strongly suggest that Wnt signal activation is not directly related to its cellular senescence and that AMBMP has binding proteins responsible for inducing cellular senescence.

### **Pathway profiling database identifies tubulin as a target protein of AMBMP**

To identify an AMBMP target molecule, I compared the cellular assays with my pathway profiling database and calculated each Pearson's correlation coefficient (activity versus activity) between AMBMP and other all compounds in my database. As a result, 12 compounds demonstrated values above 0.8, which indicated high similarities (Figure 5A). Moreover, 10 of the 12 compounds involved classical tubulin disruptors such as nocodazole (Figure 2) and were thus known from previous reports to bind to tubulin [63-65]. Of these 10 compounds, only 2, KF 38789 and chromeceptin, had not been reported to induce tubulin depolymerization. The analyzed data allowed me to predict that AMBMP would directly interact with tubulin. To test this hypothesis, I measured the tubulin disruption activity of AMBMP in a tubulin polymerization assay. Consequently, tubulin polymerization was detected by fluorescence enhancement following uptake of a fluorescent reporter molecule into the polymerized tubulin during polymerization [66].

I observed tubulin polymerization inhibition by AMBMP and nocodazole with IC<sub>50</sub> values of 0.33  $\mu$ M and 0.34  $\mu$ M, respectively (Figure 5B, Figure 6A). In this fluorescence-based polymerization assay, AMBMP was confirmed not to mediate the fluorescence interference through the observation of its UV-vis and fluorescence spectrum (Figure 7). In addition, intrinsic fluorescence quenching was used to study the potential interaction between AMBMP and tubulin. The fluorescence intensity of tubulin was decreased gradually with increasing concentrations of AMBMP, confirming its binding to tubulin. (Figure 5C). To determine the effects of these 2 compounds on the cellular microtubule network, I conducted a cell-based assay using cellular imaging techniques and fluorescent staining of tubulin. In the confocal image analysis, AMBMP and nocodazole were observed to clearly disrupt the intracellular microtubule network compared to control and SB216763-treated cells (Figure 8A). Disturbance of the microtubule network by AMBMP and nocodazole was detected with IC<sub>50</sub>

values of 0.34  $\mu\text{M}$  and 1.7  $\mu\text{M}$ , respectively (Figure 6B). Furthermore, AMBMP as well as nocodazole was observed to inhibit cell proliferation and induce a cell cycle arrest in MDA-MB-231 cells (Figure 9A, 9B). The effect of AMBMP on mitotic spindles was also observed with slightly shortening the spindle and astral microtubule at the low concentration of 30 nM and with significantly disrupting mitotic spindles at the higher concentrations of 0.3 and 3  $\mu\text{M}$  (Figure 8B), which was consistent with previous reports showing the effect of microtubule disruptors on mitotic spindles [67]. These results indicate that AMBMP had a strong inhibitory effect on tubulin polymerization, comparable to that of nocodazole. In addition, I had previously observed in my screening campaign that common tubulin disruptors induce cellular senescence (Figure 3C) [68, 69].

## Discussion

In my study, the pathway profiling database based on the biological activities of compounds was confirmed to lead to classifications corresponding to both their structural similarities and their MOAs. Through operating the system, I will both maintain and obtain data at a lower cost and in a shorter period than the HTS-FP database and BioMAP™ (DiscoverX), in which primary cells were utilized. However, my prediction method is limited to the range of target molecules of the reference compounds; however, to overcome this limitation, I will add various reference data for compounds that affect different types of target proteins other than those of the current compounds. In general, the accuracy of clustering analysis increases with a larger collection of datasets. Therefore, I will expand the cellular assays in the pathway profiling database to improve the accuracies of predicting both target molecules and cellular signaling properties. With these improvements in my system, I am attempting to perform target identification of other compounds, including my in-house compounds, with unknown targets.

In addition, I estimated the extent of cellular signaling pathways covered by my database through a computational approach. With Reactome Pathway Database [70], my pathway profiling database has the potential to detect cellular events involved in more than 200 canonical biological pathways. Moreover, 70% of the tested compounds with well-characterized MOAs had detectable activity in at least one assay in my database. Consequently, my simple system is a promising and cost-effective tool for profiling phenotypes and for predicting molecular targets of hit compounds from PDD.

By applying my profiling system for target identification of AMBMP, I have revealed that AMBMP is a tubulin disrupting molecule for the first time since the compound was reported as a Wnt agonist. The Tanimoto similarities between AMBMP and tubulin disruptors ranged from 0.12 to 0.26 (Figure 5A), which means that these compounds are apparently not structural analogs of AMBMP.

Because of their low scores, the structural similarities did not lead me to hypothesize whether AMBMP could inhibit tubulin polymerization. The achievement of AMBMP target identification supports the result that my pathway profiling database was extremely useful for predicting various pharmacological targets of compounds with unknown mechanisms. On the other hand, I consider that it is important to reveal the molecular mechanisms inhibiting tubulin polymerization by AMBMP. To address the issue, in future study, I will clarify its binding site on tubulin through a cocrystal structural analysis for AMBMP and tubulin complex.

Chemical probes are widely used to demonstrate target molecule proof-of-concept in drug discovery [71]. To this end, the selectivity of chemical probes against the intended targets is a key factor. If these chemical probes interact with unintentional molecules and induce cellular phenotypes through their off-target effects, then both time and money might be lost in the process of drug discovery research. Some past research that used AMBMP as a chemical probe for Wnt signal activation might have incorrectly generated misleading results due to inhibition of tubulin activity. Recently, the met proto-oncogene (c-MET) inhibitor tivantinib was confirmed to inhibit tubulin polymerization as well as AMBMP [72]. Through my study, KF 38789 and chromeceptin were also shown to have similar bioactive profiles to tubulin disruptors (Figure 5B), generating the possibility that both compounds interact with tubulin. These compounds will be the subject of a future publication. In addition, a previous report revealed that the structural similarities of compounds do not provide sufficient information to speculate on their biological activities [73]. For an efficient drug discovery process, it is important to evaluate and profile chemical probes using various types of cellular assays, such as my pathway profiling database.

## **Conclusion**

My pathway profiling database determined tubulin to be a target of AMBMP, which was unknown since the discovery of AMBMP, and my simple and efficient system proved to be a powerful method for predicting compound MOAs. AMBMP has been widely used as a chemical probe for Wnt signal activation, but the results for studies that used the compound might have been influenced by its modulation of tubulin activity and not Wnt signal activity. For proper utilization of chemical probes, it is potentially valuable to investigate their cellular profiles using multiple cellular assays, such my pathway profiling database, which provides beneficial information about representative cellular signaling processes. Moreover, in drug discovery, off-target interactions are strongly thought to lead to low efficacy and significant side effects in clinical trials; therefore, the development of target identification and prediction methods is now definitively required to determine not only on-target molecules but also off-target molecules. The system will certainly keep providing us with useful information for various stages of the drug discovery process through target prediction and drug safety research.

## **Methods**

### **Chemical compounds**

Tocriscreen (TOCRIS Bioscience), Natural Product Library (ENZO Life Sciences), and StemSelect Small Molecule Regulators (Merck Millipore) were all dissolved in DMSO (10 mM for Tocriscreen and StemSelect and 10 mg/mL for the Natural Product Library). AMBMP was obtained from Merck Millipore. Sodium butyrate, nocodazole, and SB216763 were sourced from Wako.

### **Cell cultures**

HEK293T, MRC5, A549, PC3, LNCaP, Jurkat, MDA-MB231, NIH-3T3, and SW480 cells were purchased from ATCC. HEK293T, A549, MRC5, and MDA-MB-231 cells were cultured in DMEM containing 4.5 g/L glucose, 10% fetal bovine serum (FBS), and penicillin/streptomycin. Jurkat, LNCaP, SW480, and PC3 cells were cultured in RPMI 1640 media containing 10% FBS and penicillin/streptomycin. NIH-3T3 cells were cultured in DMEM containing 1.5 g/L glucose, 10% FBS, and penicillin/streptomycin. All cell culture reagents were purchased from Wako.

### **Reporter gene assays in pathway profiling**

I developed reporter gene assays using a firefly luciferase system purchased from Promega. Detailed assay conditions such as cell lines, cell densities, corresponding ligands, incubation time with compounds, and materials are shown (Table 2). All assays were performed in a 384-well plate format. Plasmids were constructed by inserting each response element sequence at a multi-cloning site upstream from firefly luciferase. Transient transfections of all plasmids were performed in corresponding cell lines with Fugene HD (Promega) according to the manufacturer's instructions. In each assay, we validated the assay condition with its ligand to perform a stable screening campaign (data not shown). In all assays, all compounds were diluted in complete media at a concentration of 3

$\mu\text{g/mL}$  (Natural Product Library) and  $3 \mu\text{M}$  (other libraries) and treated for the appropriate durations. After the addition of Steady-Glo (Promega) according to the manufacturer's instructions, luminescence signals were measured using a luminescence plate reader (EnVision; PerkinElmer). We typically obtained 2 parameters calculated from each assay: one was the compound's inhibitory activity with ligand activation and the other was its agonistic activity without ligand activation.

### **Cellular proliferation assays used in pathway profiling**

Cell lines, cell densities, and incubation times with compounds are shown (Table 3). Cellular proliferation was detected with CellTiter-Glo (Promega). All assays were performed in a 384-well plate format. Luminescence signals were readout using a luminescence plate reader (EnVision; PerkinElmer). The proliferation assays with HEK293T cells and Jurkat cells were used as the counter-screen against reporter gene assays.

### **Cell-based phenotypic assays for cellular senescence inducers**

MDA-MB231 cells were seeded in a 384-well plate (3,000 cells/well) for 20 h before the treatment of compounds. After seeding, the tested compounds were diluted in complete media and incubated with cells for 24 h, followed by cytosol and nuclear staining for 1 h with CellTracker Green CMFDA and Hoechst 33342 (Invitrogen), respectively. For cellular tubulin staining, tubulin tracker green was used according to the manufacturer's instructions (Invitrogen). Cellular images were recorded with an IN Cell Analyzer 6000 (GE Healthcare). After obtaining the images, the nuclear locations and cellular areas were stained with Hoechst 33342 and CMFDA, respectively, and quantitative signals from the images were calculated using a custom-made image analysis algorithm with IN Cell Developer Toolbox (GE Healthcare).

### **Cluster analysis in the pathway profiling system**

All compounds were utilized at a concentration of 3  $\mu\text{g/mL}$  (Natural Product Library) or 3  $\mu\text{M}$  (other libraries) in the pathway profiling assays. All calculated data, including percent inhibition and percent activation number, were first normalized in each assay using the Z-scoring method and then analyzed by hierarchical clustering analysis (Ward's method) with TIBCO Spotfire software (TIBCO).

### **Calculating Pearson's correlation coefficients**

Pearson's correlation coefficients ( $R_p$ ) were calculated using the following equation:

$$R_p = \frac{\sum_{i=1}^N (x_i - \bar{x})(y_i - \bar{y})}{\sqrt{\sum_{i=1}^N (x_i - \bar{x})^2} \sqrt{\sum_{i=1}^N (y_i - \bar{y})^2}}$$

where N equals 39 assay results and  $x_i$  and  $y_i$  are the activity values of each assay in my pathway profiling database for compounds A and B, respectively.

### **Tubulin polymerization assay**

Tubulin polymerization was performed using a tubulin polymerization assay kit (BK011P, Cytoskeleton). Compounds were evaluated according to the manufacturer's instructions.

### **Tubulin binding assay with its intrinsic tryptophan fluorescence**

4  $\mu\text{M}$  of purified tubulin (Cytoskeleton) dissolved in general tubulin buffer (80 mM PIPES, pH 6.9, 2 mM  $\text{MgCl}_2$ , 0.5 mM EGTA) was pretreated with certain concentrations of compounds for 30 min. The intrinsic fluorescence spectra (320 – 400 nm) was measured with a fluorescence plate reader (EnVision; PerkinElmer) with the excitation wavelength 295 nm.

### **Immunofluorescence microscopy**

MDA-MB231 cells were incubated with compounds for 6 hours and 24 hours to observe the cellular microtubule network and the mitotic spindles respectively. Thereafter, the cells were fixed and permeabilized as described in the past report [74]. After blocking nonspecific binding with 1% donkey serum/PBS, the cells were incubated with the mouse monoclonal anti- $\beta$ -tubulin antibody (Cell Signaling Technology) (1:1000 dilution) followed by the Alexa-488 conjugated anti-mouse IgG antibody (Invitrogen) (1:500 dilution). To visualize nuclei, the cells were incubated with Hoechst33342. For staining phospho-Histone H3, the fixed cells were treated with the rabbit monoclonal anti-phospho-Histone H3 (Ser10) antibody (Cell Signaling Technology) (1:1000 dilution) followed by the Alexa-594 conjugated anti rabbit IgG antibody (Invitrogen) (1:500 dilution). Cellular images were obtained with SP8 confocal microscopy (Leica).

### **Flow cytometric analysis**

MDA-MB-231 cells were treated with compounds for 24 hours and fixed with ethanol. After fixation, cells were washed with PBS containing 2% FCS, and, subsequently, treated with Guava Cell Cycle reagent (Merck Millipore) according to the manufacturer's instructions. The DNA contents were determined using a Guava easyCyte HT software (Merck Millipore).

## **Tables and Figures**

**Table 1.** Constituents of the pathway profiling database. The types of cellular signals for the reporter gene assays and cell lines of the proliferation assays are shown.

Cellular reporter gene assays

Cellular proliferation assays

cAMP response element (CRE) signal	HEK293T
Nuclear factor of activated T-cells (NFAT) signal	MRC5
Nuclear factor kappa- light-chain-enhancer of activated B cells (NF-kB) signal	MRC5
Serum response element (SRE) signal	A549
Serum response factor (SRF) signal	PC3
p53 signal	LNCaP
E2F signal	Jurkat
Activating transcription factor 6 signal	MDA-MB-231
Hedgehog signal	
Hypoxia-inducible factor 1 (HIF1) signal	
Nuclear factor erythroid 2-related factor 2 (Nrf2) signal	
SMAD signal	
Wnt signal	

**Table 2.** Assay conditions such as cell lines, cell densities, corresponding ligands, incubation time with compounds, and materials for reporter gene assays in pathway profiling.

<b>Cellular signal</b>	<b>Cell lines</b>	<b>Cell density (cells/well)</b>	<b>Ligand</b>	<b>Incubation time with compounds</b>	<b>Original materials or references</b>
cAMP response element (CRE) signal	HEK293T	5,000	Forskolin (1 $\mu$ M)	5 h	pGL4.29 (Promega)
Nuclear factor of activated T-cells (NFAT) signal	HEK293T	5,000	Ionomycin (1 $\mu$ M)  PMA (10 ng/mL)	5 h	pGL4.30 (Promega)
Nuclear factor kappa-light-chain-enhancer of activated B cells (NF- $\kappa$ B) signal	HEK293T	10,000	TNF $\alpha$ (3 ng/mL)	20 h	pGL4.32 (Promega)
Serum response element (SRE) signal	HEK293T	20,000	FBS (15 %)  PMA (30 ng/mL)	20 h	pGL4.33 (Promega)
Serum response factor (SRF) signal	HEK293T	20,000	FBS (15 %)	5 h	pGL4.34 (Promega)
p53 signal	HEK293T	10,000	Doxorubicin  (1 $\mu$ M)	20 h	[75]

E2F signal	HEK293T	20,000	FBS (15%)	20 h	[76]
Activating transcription factor 6 signal	HEK293T	5,000	Thapsigargin (30 nM)	5 h	[77]
Hedgehog signal	NIH3T3	7,500	mouse sonic hedgehog	20 h	[78]
Hypoxia-inducible factor 1 (HIF1) signal	HEK293T	10,000	hypoxia	20 h	[79]
Nuclear factor erythroid 2-related factor 2 (Nrf2) signal	HEK293T	5,000	tert-butylhydroquinone (20 $\mu$ M)	20 h	pGL4.37 (Promega)
SMAD signal	HEK293T	10,000	TGF $\beta$ (0.2 ng/mL)	20 h	[80]
Wnt signal	HEK293T	10,000	Wnt3a	20 h	[81]
Wnt signal	SW480	10,000	no ligand (constitutive active)	20 h	[81]
IL17 signal	Jurkat	5,000	Ionomycin (400 nM)  PMA (4 ng/mL)	5 h	[82]

**Table 3** Assay conditions such as cell lines, cell densities, and incubation times for cellular proliferation assays in pathway profiling.

<b>Cell lines</b>	<b>Cell density (cells/well)</b>	<b>Incubation time with compounds</b>
HEK293T	5,000	20 h
Jurkat	5,000	20 h
MRC5	1,000	72 h
MRC5	3,500	72 h
A549	1,000	72 h
PC3	1,000	72 h
LNCaP	600	72 h
MDA-MB-231	500	72 h

**Figure 1.** Analysis of the pathway profiling database. (A) The heat map was visualized with TIBCO Spotfire software for clustering analysis. This figure represents the entire heat map of the pathway profiling database. The activities of each assay are displayed as a gradient from minimum activities (blue) to maximum activities (red). For details of the assay lists, see Table 1. (B) This cluster contained forskolin derived from each commercial compound library and NECA, a potent adenosine receptor agonist. (C) PMA and its structural analogs were grouped in the cluster shown. (D) The Tanimoto structural similarities and Pearson's correlation coefficients (activity versus activity) were calculated for PDE4 inhibitors.

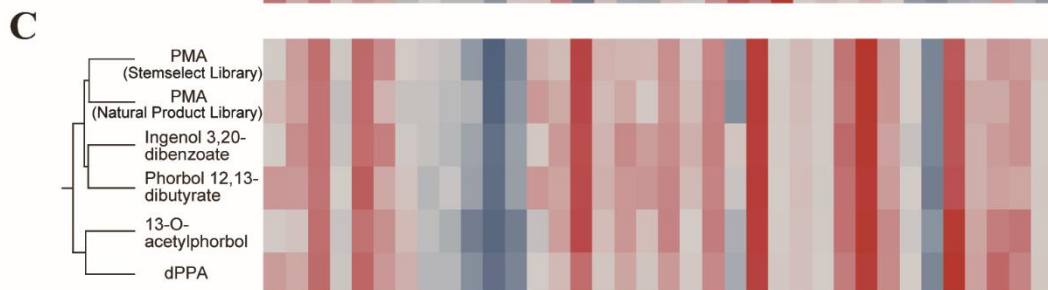
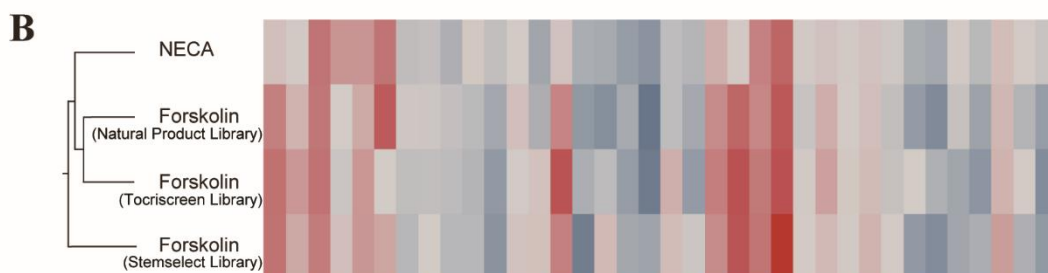
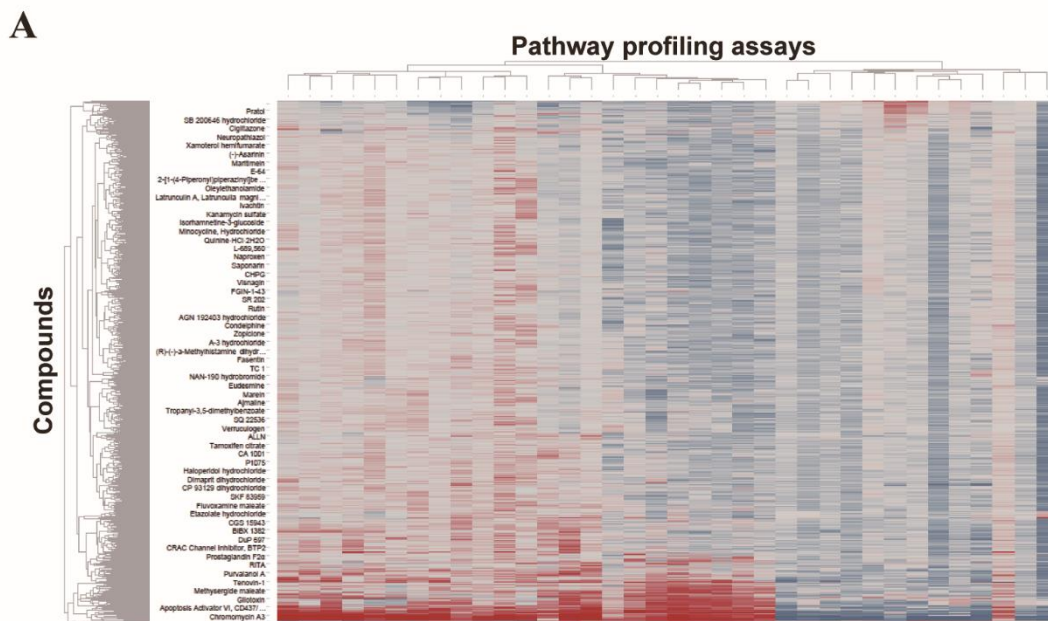
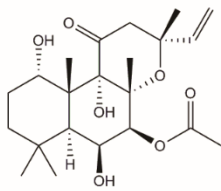
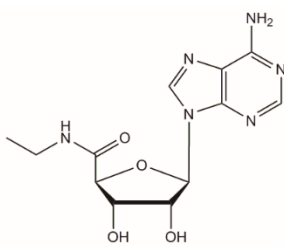


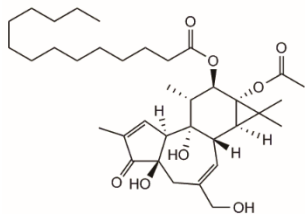
**Figure 2.** Chemical structures of the compounds discussed in this study.



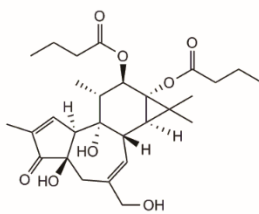
Forskolin



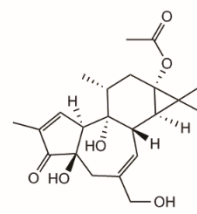
NECA



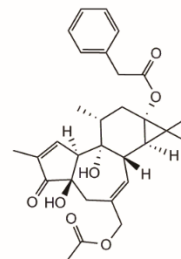
PMA



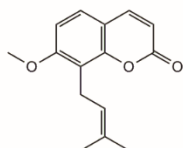
Phorbol 12,13-dibutyrate



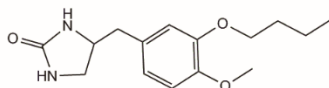
13-O-acetylphorbol



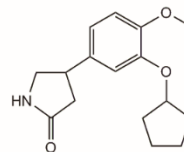
dPPA



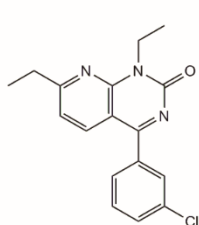
Osthole



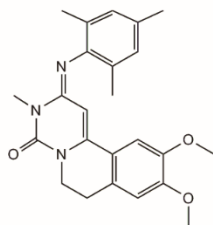
Ro20-1724



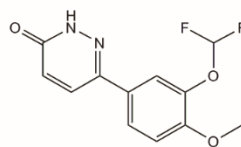
Rolipram



YM976

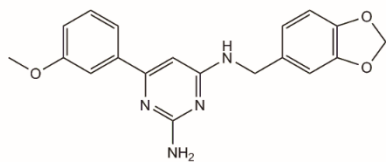


Trequinsin

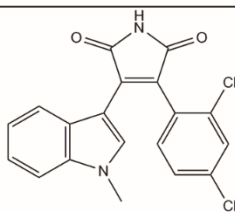


Zardaverine

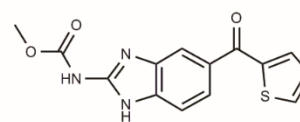
**PDE4 inhibitors**



AMBMP

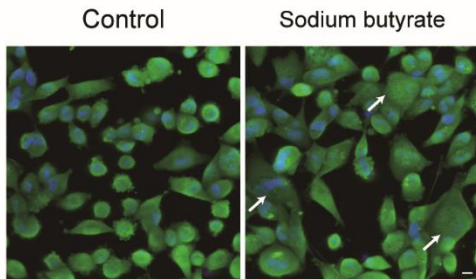


SB216763



Nocodazole

**Figure 3.** A cell-based assay for a screening campaign of cellular senescence morphology inducers by fluorescence microscopy. (A) MDA-MB231 cells were treated with 1 mM sodium butyrate. Hoechst 33342 was used as a nuclear marker (blue) and CMFDA was used to mark cytosols (green). Scale bar, 10  $\mu$ m. (B) A compound selection scheme for the discovery of senescence inducers. AMBMP was obtained as a hit compound through the screening campaign. (C) Hit compound results from the screening campaign. Fold changes in the cellular area at 3  $\mu$ M concentrations were calculated for the compounds with a custom-made image analysis algorithm. (D) Activity of the Wnt reporter gene assay with a potent GSK3 $\beta$  inhibitor, SB216763, and AMBMP is shown. The results are the mean of 3 replicate experiments (mean  $\pm$  SD). (E) MDA-MB231 cells were treated with 3  $\mu$ M SB216763, 3  $\mu$ M AMBMP, and 1 mM sodium butyrate. Hoechst 33342 was used as a nuclear marker (blue) and CMFDA was used to mark cytosols (green). Scale bar, 10  $\mu$ m.

**A****B**

Tocirscreen library: 1105 compounds  
Stemselect library: 303 compounds

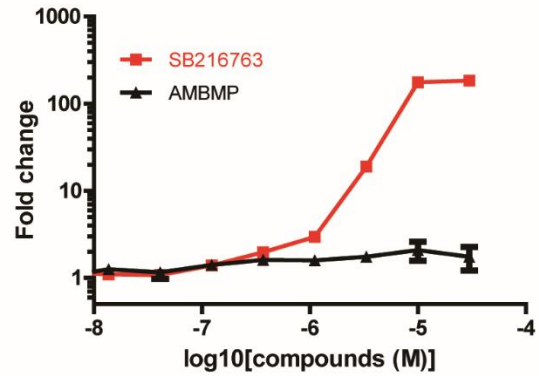
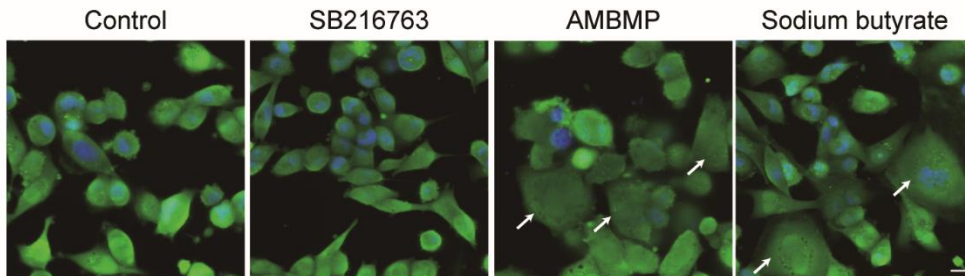
> 200% activity of cytosolic expansion @ 3  $\mu$ M  
exclude compounds decreasing cell numbers

20 compounds

AMBMP was revealed as a hit compound

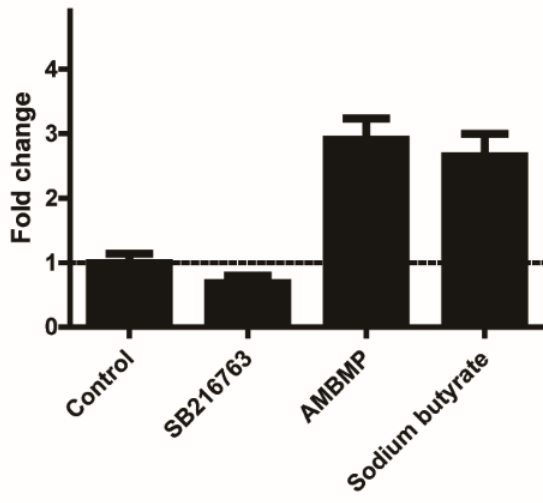
**C**

Compound name	Fold change
Nocodazole	4.1
Y-29794	4.0
ZM 447439	3.6
CMPD1	3.5
XRP44X	3.4
SCH 79797	3.4
Vincristine sulfate	3.4
Etoposide	3.3
Chromoeceptin	3.3
Reversine	3.3
<b>AMBMP</b>	<b>3.3</b>
Colchicine	3.1
Vinblastine sulfate	3.1
SB 225002	3.0
CPT 11	2.9
T113242	2.9
SN 38	2.3
Methysergide maleate	2.3
Taxol	2.2
(+)-SK&F 10047 hydrochloride	2.0

**D****E**

**Figure 4.** Measurements of fold changes in the cellular area

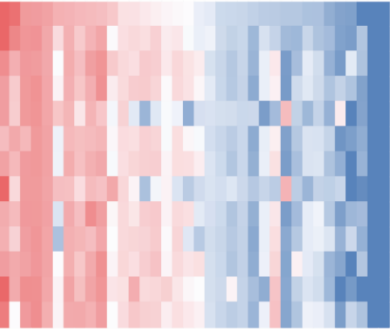
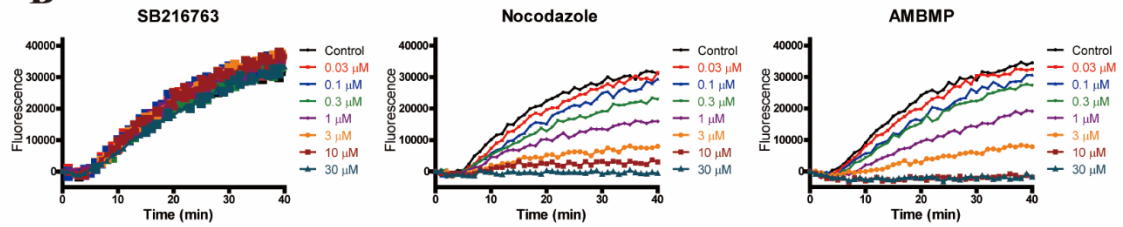
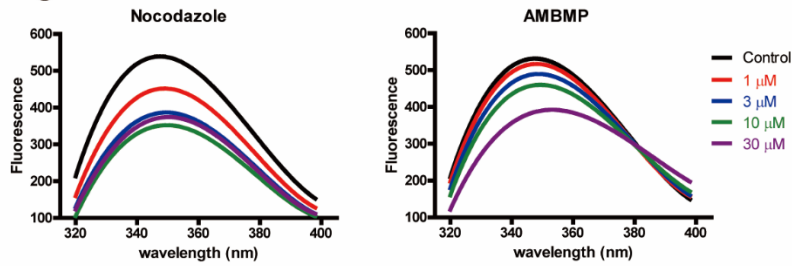
MDA-MB231 cells were treated with 3  $\mu$ M SB216763, 3  $\mu$ M AMBMP, and 1 mM sodium butyrate. To measure the cellular area, cell cytosol was stained with CMFDA and detected by IN Cell Analyzer 6000 (GE Healthcare). Fold changes in the cellular area were calculated using a custom-made image analysis algorithm with IN Cell Developer Toolbox (GE Healthcare). The results are the mean of 2 replicate experiments (means  $\pm$  SD).



**Figure 5.** Target identification of AMBMP and its binding activity to tubulin. (A) The Tanimoto structural similarities and Pearson's correlation coefficients (activity versus activity) were calculated against AMBMP. (B) SB216763, AMBMP, and nocodazole were evaluated in a tubulin polymerization assay. The results are the mean of 3 replicate experiments (with SD not shown for graphical simplicity). (C) AMBMP induced intrinsic tryptophan fluorescence spectra changes of tubulin. The results are the mean of 3 replicate experiments (with SD not shown for graphical simplicity).

**A**

Pearson Tanimoto		Compound	Biological activity
-	-	Wnt Agonist	Wnt signal activator
0.93	0.24	Nocodazole	Tubulin polymerization inhibitor
0.90	0.20	Vincristine sulfate	Tubulin polymerization inhibitor
0.90	0.24	Colchicine	Tubulin polymerization inhibitor
0.89	0.21	D-64131	Tubulin polymerization inhibitor
0.88	0.26	4'-Demethylpodophyllotoxin	Tubulin polymerization inhibitor
0.87	0.21	Vinorelbine	Tubulin polymerization inhibitor
0.85	0.16	KF 38789	Inhibitor of P-selectin-mediated cell adhesion
0.84	0.20	Vinblastine sulfate	Tubulin polymerization inhibitor
0.84	0.22	Chromoeceptin	Insulin-like growth factor 2 signal inhibitor
0.83	0.26	Podophyllotoxin	Tubulin polymerization inhibitor
0.82	0.12	T113242	Tubulin polymerization inhibitor
0.82	0.23	JK184	Hedgehog signal activator


**B****C**

**Figure 6.** Inhibitory activity on the tubulin polymerization and the cellular microtubule network

(A) IC<sub>50</sub> values of SB216763, AMBMP, and nocodazole were determined in a tubulin polymerization assay. The values were calculated using GraphPad Prism (GraphPad Software). (B) The fluorescence intensities of tubulin stained with a tubulin tracker (Invitrogen) were measured by IN Cell Analyzer 6000. IC<sub>50</sub> values of SB216763, AMBMP, and nocodazole were determined using a custom-made image analysis algorithm with IN Cell Developer Toolbox. The values were calculated by GraphPad Prism. Both results are the mean of 3 replicate experiments (mean ± SD).

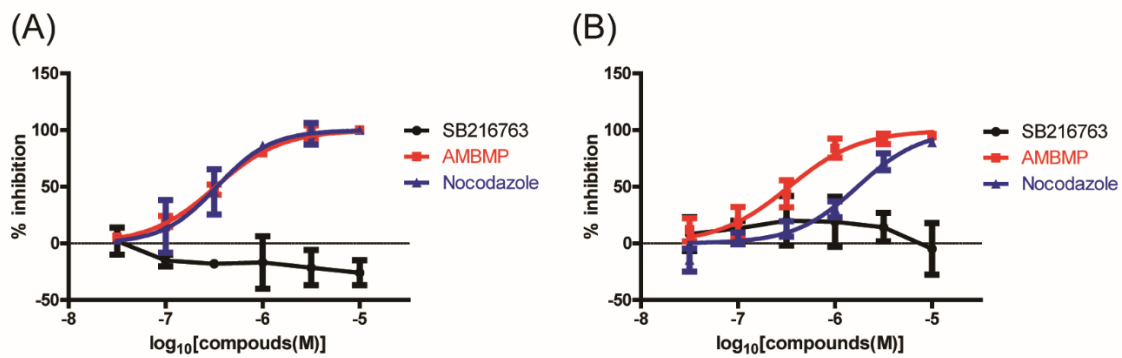
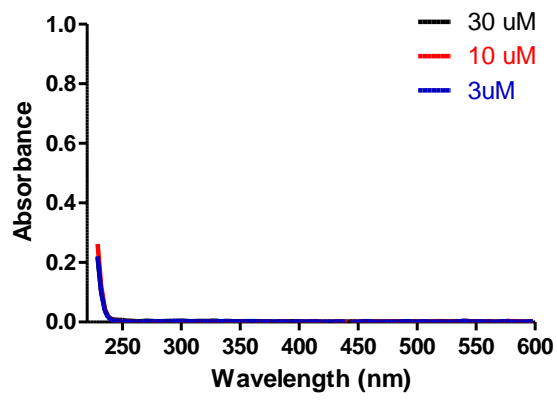


**Figure 7.** The absorbance and fluorescence profiles of AMBMP.

(A) UV-Vis spectra of AMBMP were observed with NanoDrop 1000 (Thermo Fisher Scientific).

(B) Emission spectra of AMBMP. The excitation wavelength was 350 nm and emission spectra were acquired by scanning from 380 to 500 nm using EnVision (Perkinelmer).

(A)



(B)

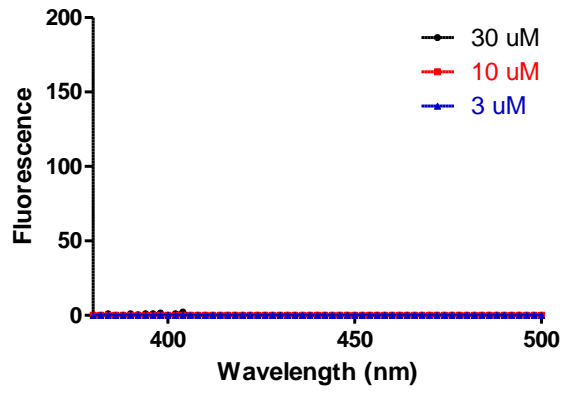
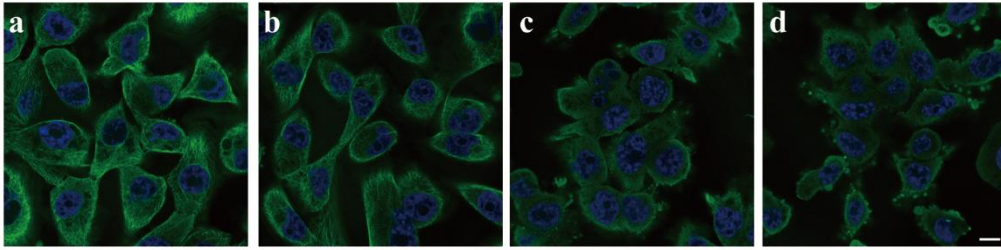


**Figure 8.** Effect of AMBMP on the cellular tubulin network and mitotic spindles. (A) The cellular tubulin network (green) was observed by fluorescence microscopy. Hoechst 33342 was used as a nuclear marker (blue). (a) control. (b) 3  $\mu$ M SB216763. (c) 3  $\mu$ M AMBMP. (d) 3  $\mu$ M Nocodazole. Scale bar, 10  $\mu$ m. (B) Control and compounds-treated MDA-MB-231 cells were stained with  $\beta$ -tubulin (green), phospho-histone H3 (red), and nuclei (blue). Phosphorylation at a highly conserved serine residue (Ser10) in the histone H3 is a key marker during the mitotic phase of the cell cycle. (a) control. (b) 30 nM nocodazole. (c) 0.3  $\mu$ M nocodazole. (d) 3  $\mu$ M nocodazole. (e) 30 nM AMBMP. (f) 0.3  $\mu$ M AMBMP. (g) 3  $\mu$ M AMBMP. Scale bar, 10  $\mu$ m.

**A**



**B**

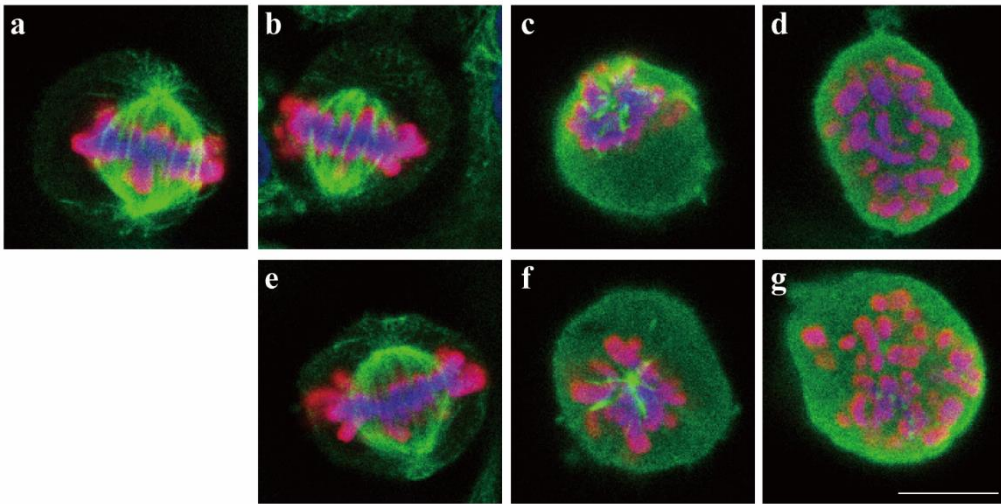
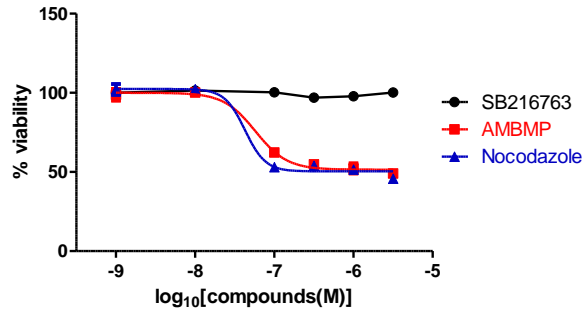


**Figure 9.** Measurements of growth inhibitory activity, cell cycle distribution, and mitotic spindle of MDA-MB231 cells treated with AMBMP

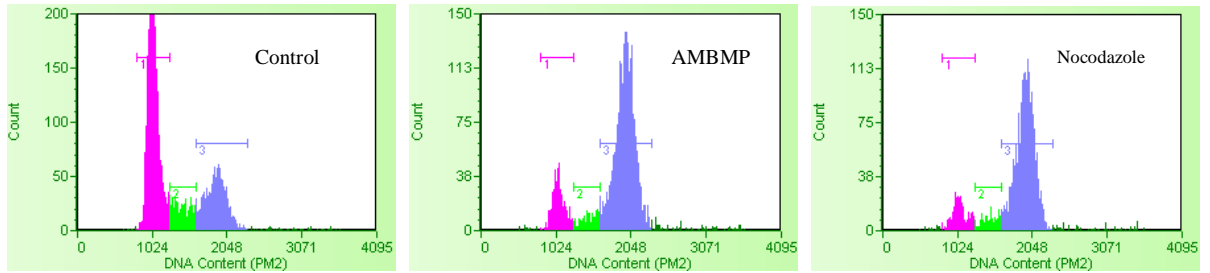
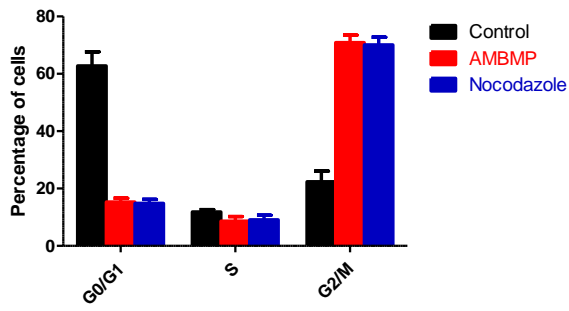
(A) The growth inhibitory activity of AMBMP and nocodazole were detected in a cell proliferation assay with the half-maximal inhibition of proliferation (IC<sub>50</sub>) values of 58 nM and 43 nM, respectively. The values were calculated using GraphPad Prism (GraphPad Software). The results are the mean of 3 replicate experiments (means  $\pm$  SD).

(B) MDA-MB-231 cells were treated with DMSO control, 3  $\mu$ M AMBMP, 3  $\mu$ M nocodazole. The cellular DNA contents were determined with flow cytometric analysis. The results are the mean of 4 replicate experiments (means  $\pm$  SD).

(A)



(B)



## **Chapter II**

### **Fluid shear stress stimulates MATE2-K expression via Nrf2 pathway activation**

## **Abstract**

Accurate prediction of drug-induced renal toxicity is necessary for development of safer drugs for patients. Cellular assay systems that recapitulate physiologically relevant microenvironments have been proposed for correct estimation of drug responses in the human body. However, establishment of such assay systems for accurate prediction of renal toxicity is challenging because of the lack of readily available in vitro assay systems. In this study, I investigated the cellular response to fluid shear stress, which is a characteristic of the environment in the kidney proximal tubules, using microfluidic devices. The global gene expression profiles of human primary proximal tubule cells under the fluidic conditions revealed upregulation of MATE2-K and activation of Nrf2 signaling in response to fluid shear stress. Network and cell biological analysis additionally showed that expression of MATE2-K is regulated by Nrf2 signaling. These results strongly suggest that fluid shear stress is involved in the expression and maintenance of function of tissue-specific drug transporters in the proximal tubule, where the cells are exposed to continuous shear stress by primary urine. Furthermore, the microfluidic culture of human proximal tubules was demonstrated to be a useful system to analyze the regulatory mechanisms of gene expression in physiologically relevant cell conditions.

## Introduction

The kidney is one of the major target organs for drug-induced toxicity, as it receives 25% of the cardiac output and is exposed to circulating xenobiotics [83]. Renal toxicity has been reported for various types of drugs such as antibiotics and anticancer agents [84, 85]. In drug development, accurate prediction of drug-induced nephrotoxicity is critical to obtain safer drugs efficiently and to reduce the costs arising from high attrition rates. Therefore, great efforts have been directed towards the improvement of predictive models for nephrotoxicity [86].

Drugs are considered to exert toxic effects against various sites within the kidney. Among them, the proximal tubule, where drug excretion, reabsorption, and accumulation occur, is considered the main target of nephrotoxicity. The proximal tubule is equipped with several important xenobiotic transporters, namely members of the solute carrier proteins (SLC) family, which mediate renal influx and efflux of compounds. Influx is mediated by the organic cation transporters 2 and the organic anion transporters 1 and 3 at the basolateral membrane of proximal tubule epithelial cells (PTECs) [87], whereas efflux is mediated at the apical membrane of PTECs by ATP-binding cassette transporters such as P-glycoprotein and multidrug resistance-associated proteins 2 and 4 [88]. The multidrug and toxin extrusion transporters 1 (MATE1, SLC47A1) and 2 (MATE2-K, SLC47A2) also play an important role in the renal excretion of drugs in the efflux phase [89]. These transport activities should be carefully considered when accurately evaluating the nephrotoxicity of drugs.

To date, drug-induced nephrotoxicity has been evaluated using kidney-derived cell lines (e.g. HK-2, OK, and MDCK) seeded on plastic plates. Although such assay systems are highly accessible and enable high throughput, they do not fully recapitulate the biological functions of human PTECs [26]. For example, the expression of mRNA for kidney-specific drug transporters in HK2 cells was reported to be much lower than that in kidney cortex tissue samples [90]. Recently, microfluidic technology has been introduced for reconstituting the physiological conditions of the proximal tubule,

such as fluid shear stress (FSS), to enable recreation of the proximal tubule with physiologically relevant toxin sensitivity and active transport of substrates [91, 92]. Furthermore, commercially available primary PTECs of human origin are easily manageable cell materials suitable for the reconstitution of human PTEC models.

In the present study, I developed physiologically relevant assay systems mimicking a FSS by using commercially available microfluidic chips, where human primary PTECs were cultured. Using the combination of microfluidic systems and human primary PTECs, I profiled the changes in gene expression under flow culture conditions relative to those under static conditions. In my study, I focused on the MATE2-K gene, as this gene plays an important role in the secretion of cationic drugs into the urine at the proximal tubules. Furthermore, bioinformatics analyses and biochemical assays were performed to show that the expression of MATE2-K was regulated by the Nrf2 pathway. To my knowledge, the mechanism underlying the expression of MATE2-K has not been revealed to date; therefore, the present study is the first report to clarify the mechanisms that regulate the expression of MATE2-K.

## **Materials and methods**

### **Chemical compounds**

Pyrimethamine, butylated hydroxyanisole, 2-acetoamidofluorene, and DAPI were obtained from Wako (Osaka, Japan). AI-1 and bardoxolone methyl were purchased from Sigma (MO, USA).

### **Cell cultures and flow culture system**

Human primary PTECs purchased from Lonza were cultured in renal epithelial basal medium (REBM, Lonza, Basel, Switzerland) with growth supplement (REGM supplement, Lonza) according to the manufacturer's instructions. PTECs were seeded on a type 4 collagen-coated  $\mu$ -slideVI 0.4 (ibidi GmbH, Bavaria, Germany) for 24 hours and subsequently cultured under FSS of 0.5 dyne/cm<sup>2</sup> using a peristaltic pump system (ATTO, Tokyo, Japan). Cells from passages two to eight were used.

### **Quantitative real-time PCR (qPCR) analysis and AmpliSeq transcriptome analysis**

Total cellular RNA was purified using an RNeasy mini kit (QIAGEN, Hilden, Germany). The purified RNA was reverse-transcribed using PrimerScript RT Master Mix (Takara, Shiga, Japan). qPCR analysis was conducted using an Applied Biosystems ABI Prism 7700 sequence detection system with TaqMan universal PCR master mix (Thermo Fisher Scientific, MA, USA). Expression levels of all genes of interest were normalized to that of cellular  $\beta$ -actin. qPCR primers and probes are shown in Table 4. In my study, human primary PTECs were characterized via Ion AmpliSeq Transcriptome gene expression analysis (Thermo Fisher Scientific), which enables the simultaneous measurement of the expression levels of over 20,000 human genes in a single assay. For AmpliSeq analysis, 10 ng of the cDNA samples was used to prepare the barcoded libraries using the Ion AmpliSeq Library Kit 2.0 (Thermo Fisher Scientific) according to the manufacturer's instructions.

### **DAPI uptake assay for measurement of MATE transport activity**

Human primary PTECs were cultured under FSS for 48 hours, followed by treatment with 100 nM DAPI (Wako) for 60 min. In this assay, all reagents were diluted in DAPI uptake assay buffer (4.7 mM KCl, 1.2 mM KH<sub>2</sub>PO<sub>4</sub>, 1.2 mM MgSO<sub>4</sub>, 2.5 mM CaCl<sub>2</sub>, 120 mM NaCl, and 25 nM NaHCO<sub>3</sub>, pH 8.0) [93]. Thereafter, to stop the assay, the cells were fixed with 4% paraformaldehyde and incubated with SYTOX green (Thermo Fisher Scientific) according to the manufacturer's instructions to visualize nuclei in all cells. We improved the assay system by using SYTOX green, which is widely used as a nuclear staining dye for accurate recognition of nuclear shape and location, with modification of the image analysis algorithm. Cellular images were recorded using the IN Cell Analyzer 6000 (GE Healthcare, IL, USA). Then, quantitative signals from the images were calculated with a custom-made image analysis algorithm using IN Cell Developer Toolbox (GE Healthcare).

### **Weighted gene co-expression network analysis (WGCNA)**

WGCNA is a method that constructs a gene network based on the similarity of expression profiles among samples, and defines modules of consistently co-expressed genes and correlates them to a trait. Co-expression network analysis was performed using the R WGCNA package [94, 95] by signed network analysis. The data set was constructed using the following method: genes with Log<sub>2</sub> RPM (read per million) values > 1 in more than 2 samples, for all samples, were only used for clustering. In the analysis, a soft-threshold power of 18, minimum module size of 30, deepSplit parameter of 0, and a merge threshold of 0.2 were used. As a result, I identified 15 modules as summarized by the eigengene (Figure 12).

### **Pathway analysis by Ingenuity Pathway Analysis (IPA)**

The 'Core Analysis' function included in IPA (QIAGEN) was used to interpret the modules in the context of biological processes, pathways, and networks.

### **Immunofluorescence microscopy**

The cells cultured under static and fluidic conditions were fixed and permeabilized as described in a previous report [74]. After blocking of nonspecific binding with 1% donkey serum/PBS, cells were incubated with a mouse monoclonal anti-heme oxygenase 1 (HO-1) antibody (Thermo Fisher Scientific) (1:100 dilution) followed by incubation with an Alexa488-conjugated anti-mouse IgG antibody (Thermo Fisher Scientific) (1:500 dilution). To visualize nuclei, cells were incubated with Hoechst33342 (Thermo Fisher Scientific). Cellular images were obtained using a SP8 confocal microscope (Leica, Wetzlar, Germany) at a magnification of 20 ×.

### **Short interfering RNA (siRNA) transfection**

KEAP1 siRNA (s18983), NRF2 siRNA (s9943), and negative control siRNA were obtained from Thermo Fisher Scientific (Silencer select pre-designed RNAi). Cells were seeded and cultured for 24 hours in growth medium. Subsequently, KEAP1- and NRF2-specific siRNA was introduced into the cells using RNAiMAX (Thermo Fisher Scientific) for 24 hours according to the manufacturer's instructions.

### **Statistical analysis**

Two-tailed Student's t-test was used to analyze difference between groups. A p-value <0.05 was considered statistically significant.

## **Results**

### **Expression profiles of PTEC-specific genes in primary PTECs under normal and fluidic culture conditions**

Under the static culture conditions as recommended in the manufacturer's instructions for primary PTECs, the expression patterns of some PTEC-specific genes such as MATE and OATs in PTECs were qualitatively different from those in intact kidney cortex tissues as observed in Body Atlas gene chip data (NextBio database) (Figure 10). In particular, the expression levels of MATE2-K and organic anion-transporting proteins (OATs) in PTECs were close to zero, in contrast to the expression in kidney cortex tissues. To elucidate the effect of FSS, I analyzed the gene expression under both static and fluidic culture conditions using AmpliSeq transcriptome analysis. My data indicate that 12 genes were highly induced, with a  $\geq 3$ -fold change in expression levels, by exposure to shear stress under fluidic conditions (Table 5). In the following study, I focused on MATE2-K because of its importance in the renal tubular secretion of cationic drugs.

### **Induction of MATE2-K expression by FSS on PTECs**

Using the present fluidic system, the expression level of MATE2-K was increased in a time-dependent manner in response to FSS by qPCR (Figure 11A). To evaluate the transport activity of MATE2-K, I established a cell-based assay using DAPI, which has been shown to be a specific substrate of MATE transporters [93]. Fluorescence image analysis revealed increased uptake of DAPI under fluidic culture conditions (Figure 11B). In addition, to confirm the MATE-dependent uptake of DAPI, I used the potent and specific MATE inhibitor pyrimethamine [96]. Pyrimethamine exerted a strong inhibitory effect on DAPI uptake (Figure 11C), suggesting that DAPI was taken up by primary PTECs through the MATE-dependent transport function. Additionally, the expression of MATE2-K was found to be increased under 24-hour fluidic conditions and then restored to baseline under

subsequent 24-hour static conditions, suggesting that MATE2-K expression is reversibly regulated by FSS (Figure 11D). These results indicate that the expression and transport activity of MATE2 are highly dependent on FSS.

### **Network analysis of global gene expression data under fluidic conditions**

To identify the mechanisms by which MATE2-K expression is regulated in fluidic cell culture, I first performed WGCNA and constructed a co-expression network for different static and fluidic culture conditions at three time points. Under the conditions of softpower threshold = 18, deepSplit = 0, all genes were classified into 15 co-expression modules (Figure 12). Some modules showed expression patterns associated with flow conditions; among them, the black module, which included MATE2-K and 891 other genes, was found to be upregulated in a flow- and time-dependent manner (Figure 13A). I next examined pathway enrichment using the IPA core analysis module. Pathway analysis revealed the Nrf2 pathway to be a potential candidate related to the black module for MATE2-K expression (Table 6), as 22 genes regulated by the Nrf2 pathway were enriched in the black module with the lowest P value (Table 6 and Figure 14). I also discovered that the mRNA expression and protein level of HO-1, a representative Nrf2-responsive gene, in PTECs were enhanced by FSS in human primary PTECs (Figure 13B, 13C). These results suggest that the Nrf2 pathway is upregulated by FSS and plays an essential role in the expression of MATE2-K.

### **Regulation of MATE2-K expression by Nrf2 signal activation**

To investigate the mechanism by which MATE2-K expression is activated by Nrf2 signaling, I measured the mRNA expression levels of MATE2-K following treatment with commonly used Nrf2 activators such as bardoxolone methyl (BARD) [97], AI-1 [98], butylated hydroxyanisole (BHA) [99], and 2-acetoamidofluorene (2-AAF) [100]. These Nrf2 activators were found to induce the expression

of MATE2-K as well as HO-1 (Figure 15A, 15B) and to elevate MATE2-K transport activity in the DAPI uptake assay (Figure 15C). In addition, I conducted loss-of-function analysis using siRNA for Kelch-like ECH associating protein 1 (KEAP1) and NRF2 to confirm the relationship between MATE2-K and the Nrf2 pathway. As previously reported [101], siRNA knockdown of KEAP1 or NRF2 increased or decreased the expression of NRF2 target genes such as HO-1. The mRNA and protein levels of KEAP1 and NRF2 following siRNA knockdown of KEAP1 or NRF2 were measured by qPCR and Western blotting, respectively (Figure 15D, 15E, and Figure 16). MATE2-K expression was highly enhanced by KEAP1 knockdown (Figure 15D) and suppressed by NRF2 knockdown (Figure 15E). Similarly, I detected changes in DAPI uptake in PTECs treated with KEAP1 or NRF2 siRNA, and confirmed that DAPI uptake mediated by MATE2-K was inhibited by pyrimethamine (Figure 15F). These results strongly indicate that Nrf2 signaling controls the expression of MATE2-K.

## Discussion

Advances in microfluidic technology have enabled the application of microfluidic devices by both engineers and biologists to elucidate the mechanisms underlying biological phenomena under biomimetic conditions [102]. An organ-on-a-chip is a widely accepted model for reconstituting cellular microenvironments using microfluidic technology [103]. Although Jang et al. developed PTEC-on-a-chip [92], they did not clarify the specific gene expression changes in these cells under microfluidic conditions. In my study, gene expression profiling in primary human PTECs under fluidic environments revealed that the expression of several genes was modulated in response to FSS (Table 5). MATE2-K, a key transporter of cationic drugs in the proximal tubules, was found to be highly upregulated in response to FSS. To date, there have been no reports describing FSS-induced upregulation of MATE2-K or its underlying mechanism. Therefore, I analyzed the upregulation of MATE2-K in response to FSS. In this study, SLC47A1 (MATE1) of the MATE family was not investigated, as its expression was found to be minimally responsive to FFS with a fold change of 1.3 under the present experimental conditions (Table 5). WGCNA, an effective analysis method for identifying gene co-expression modules, was used to reveal candidate signals related to the expression of MATE2-K. I analyzed these candidates further to identify the signal responsible for MATE2-K expression; in particular, I focused on the Nrf2 pathway as this signal showed the lowest P value (Table 6).

The Nrf2 pathway is the major regulator of cytoprotective responses to oxidative stresses caused by reactive oxygen species (ROS) and electrophiles. When this pathway is activated by stress, the transcription factor NRF2 binds the antioxidant response element in the regulatory regions of target genes [104]. The Nrf2-responsive proteins HO-1 and NQO1 have been shown to respond to FSS in vascular endothelial cells [105-107]. My results also demonstrated upregulation of HO-1 and NQO1 in response to FSS in PTECs (Table 5). To my knowledge, my study is the first to report that the

expression of these Nrf2-responsive genes is enhanced by FSS in PTECs as well as in vascular endothelial cells. A possible explanation underlying the observation of the same response to FSS in different cell types is that the similar vascular structure in both tissue types is exposed to fluid flow, i.e., primary urine in PTECs and blood in blood vessels. Although the detailed mechanisms of Nrf2 signal induction under fluidic culture are not understood, Nrf2 signaling is definitively responsible for retention of function under stresses such as ROS caused by FSS. To elucidate these detailed mechanisms, further studies are needed.

To clarify the relationship between the Nrf2 pathway and MATE2-K expression, I conducted biochemical assays using Nrf2 activators and loss-of-function analysis using siRNA. In my study, four compounds widely used as Nrf2 activators were found to increase HO-1 and MATE2-K expression. Additionally, I confirmed that MATE2-K upregulation by bardoxolone increased its transport activity in the DAPI uptake assay. Furthermore, I demonstrated that the MATE2-K expression was increased by the treatment with KEAP1 siRNA and decreased by NRF2 siRNA. These results suggest that expression of MATE2-K is regulated by the Nrf2 pathway. Recent studies have revealed that Nrf2 activation increases the expression of drug efflux pumps [108] and drug-metabolizing enzymes [109, 110], demonstrating that Nrf2 plays a possible role in regulating the genes involved in drug metabolism and disposition. Accordingly, these results imply that Nrf2 signal activation by FSS represents an important mechanism for maintaining physiological function in proximal tubules. However, I did not attempt to identify the Nrf2-binding sites in the MATE2-K promoter region in this work. I aim to perform MATE2-K promoter analysis using cell biological approaches in future studies.

In contrast, the expression of MATE1 and OATs was not increased under the present microfluidic conditions. Their transcription is reportedly regulated by hepatocyte nuclear factors (HNF) [111, 112]. Recently, the expression of HNF4 has been shown to be affected by the stiffness

of the extracellular matrix (ECM), which is a physical parameter characteristic of tissue type [113]. This finding highlights the importance of scaffold stiffness for recreating physiologically relevant in vitro models. My present system did not reconstitute appropriate ECM stiffness for PTECs. To fully recapitulate cellular microenvironments, microfluidic technology should be integrated with soft biomaterial scaffolds such as hydrogels that possess appropriate stiffness and incorporate ECM components.

In summary, I showed that FSS enhances MATE2-K expression in human primary PTECs, and that this enhanced expression results from FSS-induced Nrf2 activation. My study indicates that reconstitution of cellular microenvironments, such as physical stresses, is critical for the development of in vitro proximal tubule models to study drug-induced renal toxicity in drug discovery research.

## Tables and Figures

**Table 4.** Taqman probes for qPCR analysis

Species	Assay	Assay ID
Human	<i>HO-1</i>	Hs01110250_m1
Human	<i>MATE2-K</i>	Hs00945650_m1
Human	<i>KEAP1</i>	Hs00202227_m1

**Table 5.** List of genes whose expression is FSS-responsive with a  $\geq 3$ -fold change in expression level

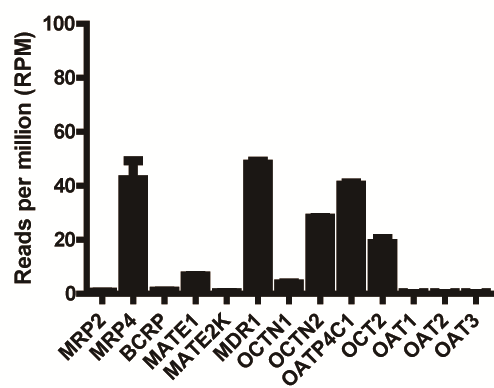
Gene symbol	Gene description	Fold change	<i>P</i> value
<i>HMOX1</i>	heme oxygenase (decycling) 1	18.1	$3.8 \times 10^{-3}$
<i>NQO1</i>	NAD(P)H dehydrogenase, quinone 1	7.4	$6.6 \times 10^{-3}$
<i>ANGPTL4</i>	angiopoietin-like 4	5.7	$7.0 \times 10^{-6}$
	solute carrier family 47 (multidrug and toxin		
<i>SLC47A2</i>	extrusion), member 2	5.3	$1.3 \times 10^{-3}$
<i>SLC44A2</i>	solute carrier family 44 (choline transporter), member 2	4.5	$1.3 \times 10^{-4}$
	semaphorin 7A, GPI membrane anchor (John Milton		
<i>SEMA7A</i>	Hagen blood group)	4.3	$1.9 \times 10^{-4}$
<i>CPT1A</i>	carnitine palmitoyltransferase 1A (liver)	3.8	$1.3 \times 10^{-3}$
<i>SRXN1</i>	sulfiredoxin 1	3.4	$7.8 \times 10^{-3}$
<i>GCLM</i>	glutamate-cysteine ligase, modifier subunit	3.3	$1.4 \times 10^{-3}$
<i>PK4</i>	pyruvate dehydrogenase kinase, isozyme 4	3.3	$1.1 \times 10^{-3}$
<i>AKR1C3</i>	aldo-keto reductase family 1, member C3	3.2	$5.0 \times 10^{-3}$
<i>GPR56</i>	G protein-coupled receptor 56	3.0	$8.7 \times 10^{-4}$
	solute carrier family 47 (multidrug and toxin		
<i>SLC47A1</i>	extrusion), member 1	1.3	$5.2 \times 10^{-1}$

**Table 6.** Candidate pathways regulating *MATE2-K* expression

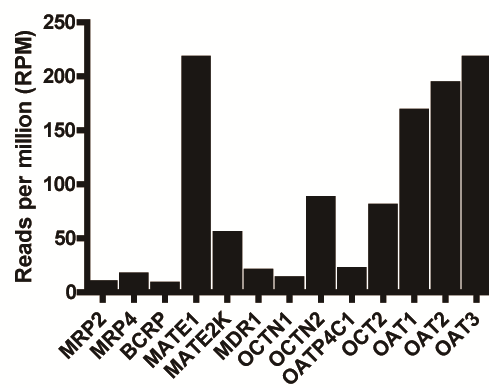
Canonical pathway	<i>P</i> value
NRF2-mediated oxidative stress response	$7.0 \times 10^{-6}$
Axonal guidance signaling	$6.9 \times 10^{-6}$
Hepatic fibrosis/hepatic stellate cell activation	$1.0 \times 10^{-5}$
Glutathione biosynthesis	$5.9 \times 10^{-5}$
Ethanol degradation IV	$3.3 \times 10^{-4}$

**Figure 10.** Gene expression levels of major transporters in the kidney cells and tissues. (A) AmpliSeq transcriptome analysis of commercially available primary PTECs under the static culture condition. The results are the mean of 3 replicate experiments; (means  $\pm$  SD). (B) Affimetrix GeneChip analysis of human kidney cortex, according to the Body Atlas in the NextBio database.

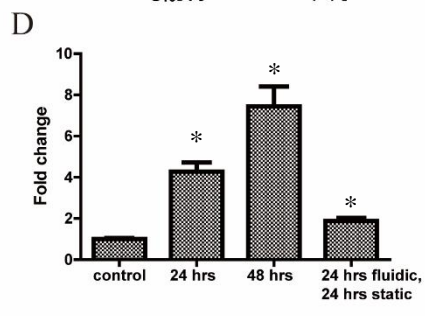
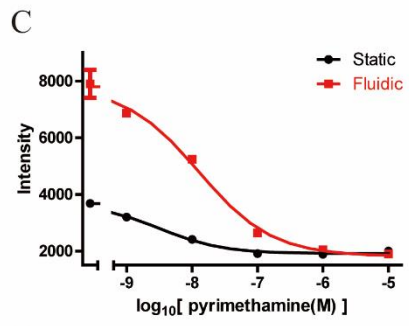
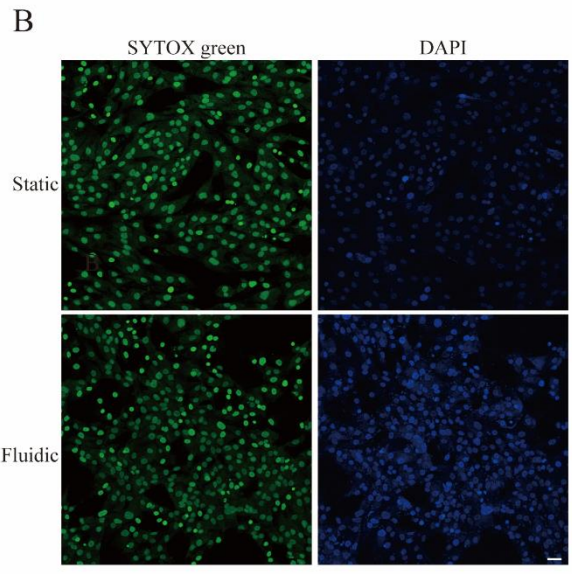
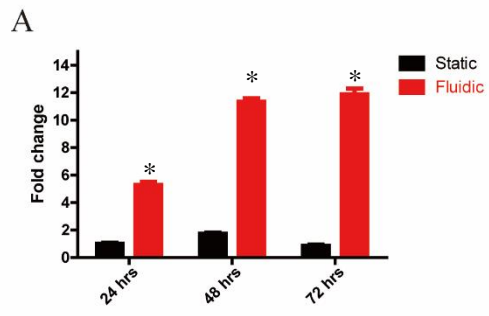
A



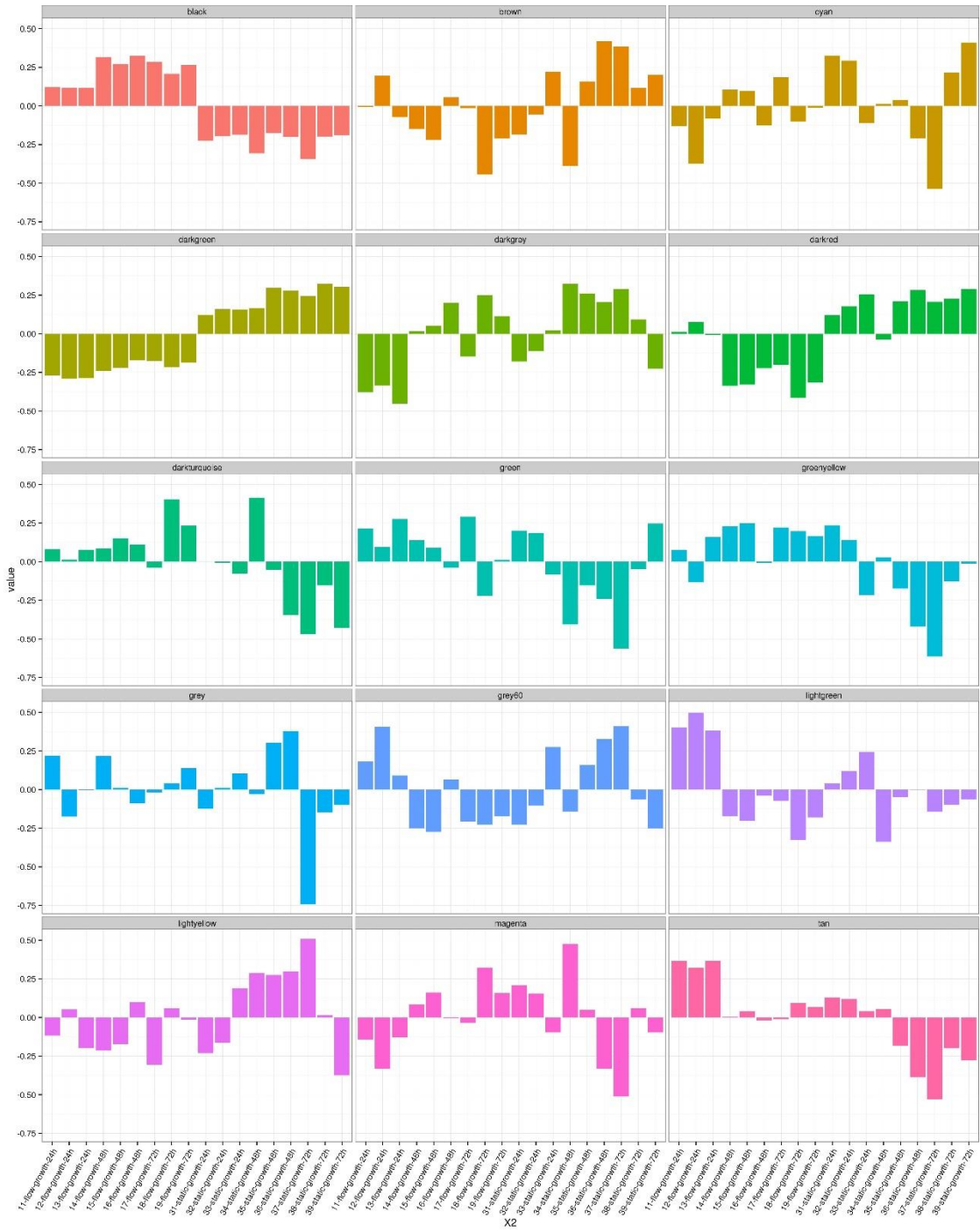
B



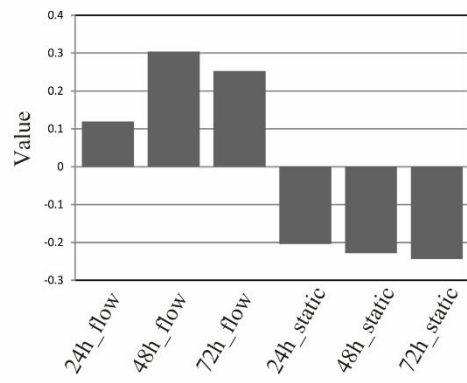
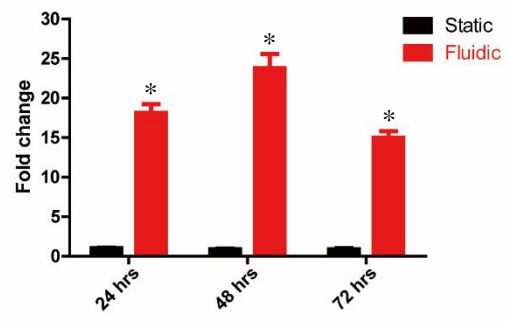
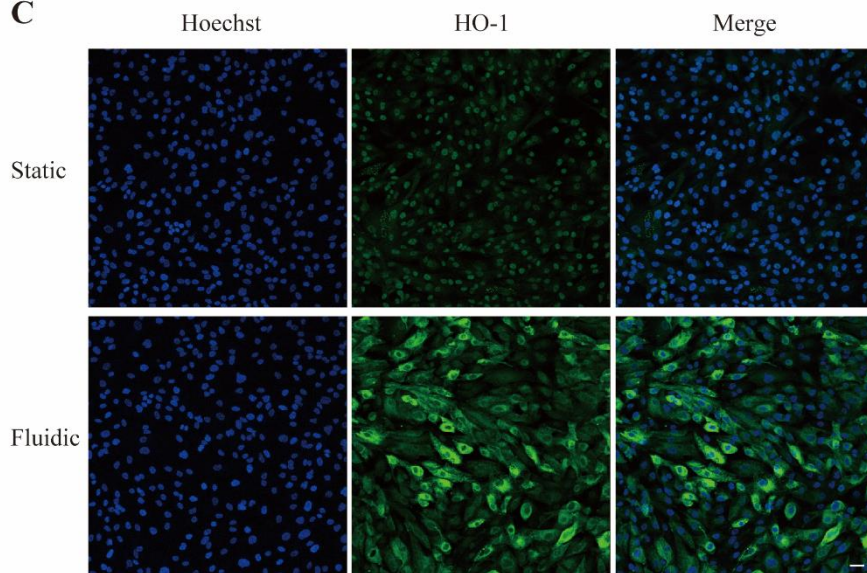
**Figure 11.** MATE2-K expression and transport activity in PTECs under the static and fluidic culture conditions. (A) MATE2-K mRNA expression changes in PTECs cultured in the microfluidic system compared to those in the static condition. The expression levels were analyzed by qPCR and fold changes were normalized to the levels in static control samples. (B) MATE2-K transport activity was evaluated by DAPI uptake assay. Scale bar, 50  $\mu$ m. (C) Pyrimethamine, a MATE-specific inhibitor, suppressed MATE2-K transport activity. DAPI uptake activity was indicated as intensity values measured by IN Cell Analyzer. (D) MATE2-K expression was reversibly modulated in response to FSS. The results shown are the value from qPCR and the mean of 3 replicate experiments (mean  $\pm$  SD). Significant difference between static and fluidic groups were represented by asterix: \* $p$ <0.01.



**Figure 12.** WGCNA classified genes into 15 co-expression modules based on their expression patterns.



**Figure 13.** Upregulation of the Nrf2 pathway under fluidic conditions. (A) The expression profiles of the eigengene for a co-expression cluster involving MATE2-K, generated by WGCNA. (B) HO-1 mRNA expression changes in PTECs cultured in the microfluidic system were significantly higher than those in cells cultured in static conditions. Fold changes were normalized to the levels in static control samples. The results are the mean of 3 replicate experiments (mean  $\pm$  SD). (C) Immunofluorescence microscopy analysis revealed FSS-induced upregulation of HO-1. Scale bar, 50  $\mu$ m. Significant difference between static and fluidic groups were represented by asterix: \* $p$ <0.01.

**A****B****C**

**Figure 14.** Pathway analysis. (A) WGCNA-derived list of Nrf2-responsive genes comprising the black module. (B) Network analysis map for the black module.

(A)

Symbol	Entrez Gene Name
<i>ABCC2</i>	ATP binding cassette subfamily C member 2
<i>ATF4</i>	activating transcription factor 4
<i>CAT</i>	catalase
<i>DNAJB5</i>	DnaJ heat shock protein family (Hsp40) member B5
<i>DNAJB7</i>	DnaJ heat shock protein family (Hsp40) member B7
<i>DNAJC11</i>	DnaJ heat shock protein family (Hsp40) member C11
<i>EPHX1</i>	epoxide hydrolase 1
<i>FTH1</i>	ferritin heavy chain 1
<i>FTL</i>	ferritin light chain
<i>GCLC</i>	glutamate-cysteine ligase catalytic subunit
<i>GCLM</i>	glutamate-cysteine ligase modifier subunit
<i>GSR</i>	glutathione-disulfide reductase
<i>GSTM4</i>	glutathione S-transferase mu 4
<i>GSTP1</i>	glutathione S-transferase pi 1
<i>HMOX1</i>	heme oxygenase 1
<i>MGST2</i>	microsomal glutathione S-transferase 2
<i>NQO1</i>	NAD(P)H quinone dehydrogenase 1
<i>PIK3CD</i>	phosphatidylinositol-4,5-bisphosphate 3-kinase catalytic subunit delta
<i>PPIB</i>	peptidylprolyl isomerase B
<i>PRDX1</i>	peroxiredoxin 1
<i>PRKCQ</i>	protein kinase C theta
<i>SQSTM1</i>	sequestosome 1

(B)

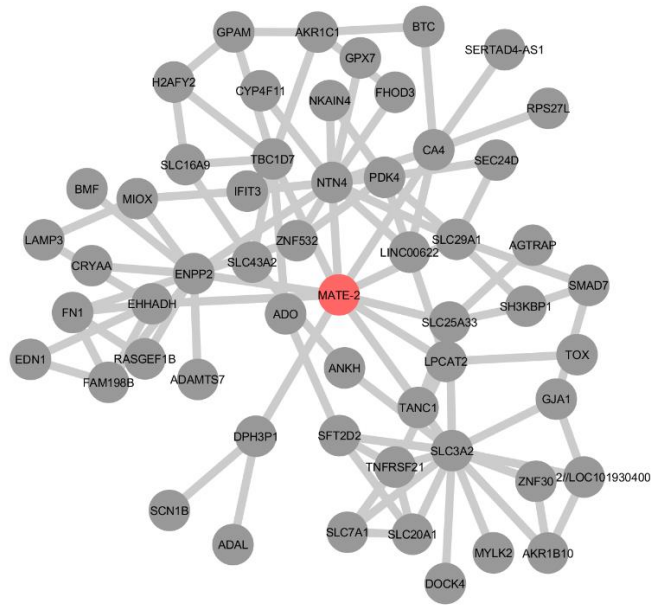


**Figure 15.** Regulation of MATE2-K expression. mRNA expression changes of HO-1 (A) and MATE2-K (B) were measured following treatment of PTEC with Nrf2 activators: AI-1 (10  $\mu$ M), BHA (100  $\mu$ M), 2-AAF (100  $\mu$ M), and BARD (10 nM) (C) Pyrimethamine suppressed MATE2-K transport activity induced by 10 nM bardoxolone. mRNA levels of KEAP1, NRF2, HO-1, and MATE2-K expression in PTEC samples following treatment with KEAP1 (D) and NRF2 (E) siRNA were determined by qPCR. (F) Pyrimethamine suppressed MATE2-K transport activity modulated by treatment with KEAP1 and NRF2 siRNA. These results are the means of 3 (A, B, C, and F) and 5 (D and E) replicate experiments (mean  $\pm$  SD). Significant difference between control and treatment groups were represented by asterix: \* $p$ <0.05, \*\* $p$ <0.01.

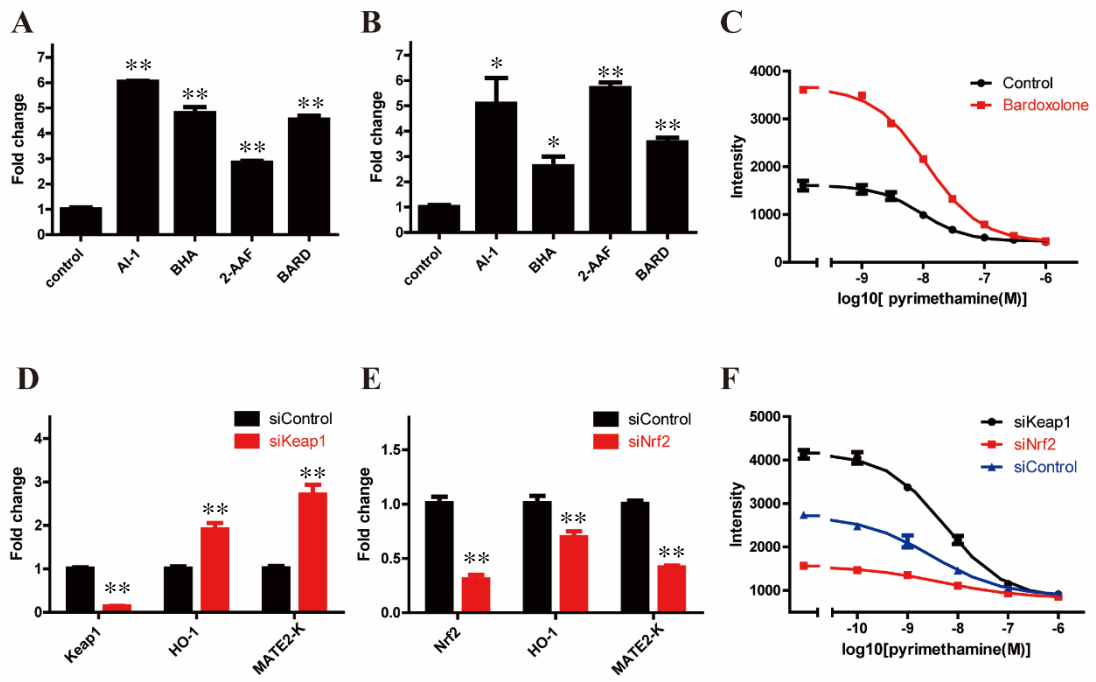
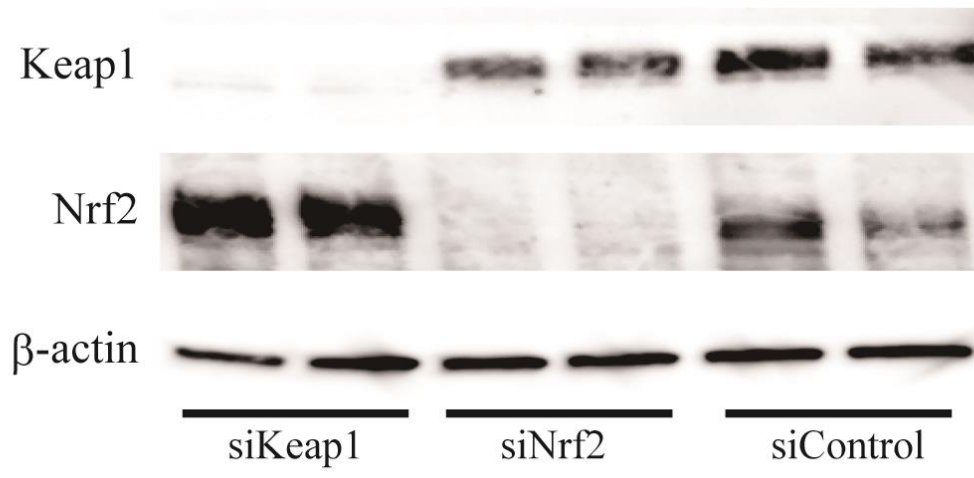


**Figure 16.** Protein expression levels of Keap1 (A), Nrf2 (B), and  $\beta$ -actin (C) following treatment with Keap1 and Nrf2 siRNAs, as determined by western blot analysis.



## **General Conclusion**

In my study, I focused on the development of research platforms to detect adverse drug effects in the early phase of drug discovery research. Non-clinical toxicity and clinical safety are critically important for the discovery of safer and more effective drugs. These aspects are also primary reasons for candidate drug terminations. To effectively and accurately detect adverse drug effects, I considered two main issues: how to identify unknown off-target molecules of drugs and how to recapitulate drug-induced responses with *in vitro* systems in laboratories. To solve these issues, I developed the pathway profiling system to easily identify drug off-target molecules (chapter I) and a physiologically relevant cellular system with PTEC (chapter II).

Currently, to improve the success rate of drug discovery, a number of researchers focus on drug toxicology because a large number of drug candidates have failed owing to safety issues. My developed platforms provide researchers with tools to detect cellular toxicities and off-target molecules, consequently contributing to the selection of appropriate drug candidates for the development of safer and more effective drugs. Moreover, although the complete human genome has been sequenced and analyzed in detail using NGS technologies, the functions of several genes have not been identified. My platforms can be applied not only to detect drug responses but also to reveal gene functions, and can be used in addition to current molecular biological methods, such as gene-editing technologies.

## **Acknowledgement**

I am deeply grateful to Professors Kazuto Nakada, Hiroshi Wada, and Tomoki Chiba and Associate Professor Hidekazu Kuwayama for guiding my work and valuable discussions through my doctoral program.

I am very thankful to Dr. Osamu Sano, Dr. Kenichi Kazetani, Mr. Koji Yamamoto, Dr. Hidehisa Iwata, Mr. Junji Matsui, Dr. Misato Kaishima, Mr. Toshiyuki Ohnishi, Dr. Kimio Tohyama, Ms. Ikumi Chisaki, Mr. Yusuke Nakayama, Ms. Mari Ogasawara-Shimizu, Dr. Yuji Kawamata, Takeda Pharmaceutical Company, for supporting materials, valuable suggestions and comments.

Finally, I would like to appreciate my family for supporting my life in University of Tsukuba.

## References

1. Boettcher M, McManus MT: **Choosing the Right Tool for the Job: RNAi, TALEN or CRISPR.** *Molecular cell* 2015, **58**(4):575-585.
2. Frye SV: **The art of the chemical probe.** *Nature Chemical Biology* 2010, **6**:159.
3. de Torre-Minguela C, Mesa del Castillo P, Pelegrín P: **The NLRP3 and Pyrin Inflammasomes: Implications in the Pathophysiology of Autoinflammatory Diseases.** *Frontiers in Immunology* 2017, **8**(43).
4. Jesus AA, Goldbach-Mansky R: **IL-1 Blockade in Autoinflammatory Syndromes.** *Annual review of medicine* 2014, **65**:223-244.
5. Shao B-Z, Xu Z-Q, Han B-Z, Su D-F, Liu C: **NLRP3 inflammasome and its inhibitors: a review.** *Frontiers in Pharmacology* 2015, **6**:262-262.
6. Onakpoya IJ, Heneghan CJ, Aronson JK: **Post-marketing withdrawal of 462 medicinal products because of adverse drug reactions: a systematic review of the world literature.** *BMC Medicine* 2016, **14**:10.
7. Lynch JJ, Van Vleet TR, Mittelstadt SW, Blomme EAG: **Potential functional and pathological side effects related to off-target pharmacological activity.** *Journal of Pharmacological and Toxicological Methods* 2017, **87**:108-126.
8. Anighoro A, Bajorath J, Rastelli G: **Polypharmacology: Challenges and Opportunities in Drug Discovery.** *Journal of Medicinal Chemistry* 2014, **57**(19):7874-7887.
9. Cox TC: **Utility and limitations of animal models for the functional validation of human sequence variants.** *Molecular Genetics & Genomic Medicine* 2015, **3**(5):375-382.
10. van der Worp HB, Howells DW, Sena ES, Porritt MJ, Rewell S, O'Collins V, Macleod MR: **Can Animal Models of Disease Reliably Inform Human Studies?** *PLOS Medicine* 2010, **7**(3):e1000245.
11. Baillie TA, Rettie AE: **Role of Biotransformation in Drug-Induced Toxicity: Influence of Intra- and Inter-Species Differences in Drug Metabolism.** *Drug Metabolism and Pharmacokinetics* 2011, **26**(1):15-29.
12. Chu X, Bleasby K, Evers R: **Species differences in drug transporters and implications for translating preclinical findings to humans.** *Expert Opinion on Drug Metabolism & Toxicology* 2013, **9**(3):237-252.
13. Horvath P, Aulner N, Bickle M, Davies AM, Nery ED, Ebner D, Montoya MC, Östling P, Pietiäinen V, Price LS *et al*: **Screening out irrelevant cell-based models of disease.** *Nature Reviews Drug Discovery* 2016, **15**:751.
14. Kahn JD: **Connecting the dots in translational research.** *Nature Reviews Drug Discovery* 2012, **11**:811.
15. Austin CP: **Translating translation.** *Nature Reviews Drug Discovery* 2018, **17**:455.
16. Arrowsmith J, Miller P: **Trial Watch: Phase II and Phase III attrition rates 2011-2012.** *Nat*

- Rev Drug Discov* 2013, **12**(8):569-569.
17. Waring MJ, Arrowsmith J, Leach AR, Leeson PD, Mandrell S, Owen RM, Pairaudeau G, Pennie WD, Pickett SD, Wang J *et al*: **An analysis of the attrition of drug candidates from four major pharmaceutical companies.** *Nature Reviews Drug Discovery* 2015, **14**:475.
  18. Tagliatalata M, Pannaccione A, Castaldo P, Giorgio G, Zhou Z, January CT, Genovese A, Marone G, Annunziato L: **Molecular Basis for the Lack of HERG K<sup>+</sup> Channel Block-Related Cardiotoxicity by the H<sub>1</sub> Receptor Blocker Cetirizine Compared with Other Second-Generation Antihistamines.** *Molecular Pharmacology* 1998, **54**(1):113.
  19. De Hert M, Detraux J, van Winkel R, Yu W, Correll CU: **Metabolic and cardiovascular adverse effects associated with antipsychotic drugs.** *Nature Reviews Endocrinology* 2011, **8**:114.
  20. Balijepalli S, Kenchappa RS, Boyd MR, Ravindranath V: **Protein thiol oxidation by haloperidol results in inhibition of mitochondrial complex I in brain regions: comparison with atypical antipsychotics.** *Neurochemistry International* 2001, **38**(5):425-435.
  21. Lounkine E, Keiser MJ, Whitebread S, Mikhailov D, Hamon J, Jenkins JL, Lavan P, Weber E, Doak AK, Côté S *et al*: **Large-scale prediction and testing of drug activity on side-effect targets.** *Nature* 2012, **486**:361.
  22. Mayr A, Klambauer G, Unterthiner T, Hochreiter S: **DeepTox: Toxicity Prediction using Deep Learning.** *Frontiers in Environmental Science* 2016, **3**(80).
  23. Ito T, Ando H, Suzuki T, Ogura T, Hotta K, Imamura Y, Yamaguchi Y, Handa H: **Identification of a Primary Target of Thalidomide Teratogenicity.** *Science* 2010, **327**(5971):1345-1350.
  24. Rix U, Superti-Furga G: **Target profiling of small molecules by chemical proteomics.** *Nat Chem Biol* 2009, **5**(9):616-624.
  25. Petrone PM, Simms B, Nigsch F, Lounkine E, Kutchukian P, Cornett A, Deng Z, Davies JW, Jenkins JL, Glick M: **Rethinking Molecular Similarity: Comparing Compounds on the Basis of Biological Activity.** *ACS Chemical Biology* 2012, **7**(8):1399-1409.
  26. Huang JX, Kaeslin G, Ranall MV, Blaskovich MA, Becker B, Butler MS, Little MH, Lash LH, Cooper MA: **Evaluation of biomarkers for in vitro prediction of drug-induced nephrotoxicity: comparison of HK-2, immortalized human proximal tubule epithelial, and primary cultures of human proximal tubular cells.** *Pharmacology Research & Perspectives* 2015, **3**(3):e00148.
  27. Takahashi K, Yamanaka S: **Induction of Pluripotent Stem Cells from Mouse Embryonic and Adult Fibroblast Cultures by Defined Factors.** *Cell* 2006, **126**(4):663-676.
  28. Shi Y, Inoue H, Wu JC, Yamanaka S: **Induced pluripotent stem cell technology: a decade of progress.** *Nature Reviews Drug Discovery* 2016, **16**:115.

29. Okita K, Yamanaka S: **Induced pluripotent stem cells: opportunities and challenges.** *Philosophical Transactions of the Royal Society B: Biological Sciences* 2011, **366**(1575):2198-2207.
30. Saha K, Jaenisch R: **Technical Challenges in Using Human Induced Pluripotent Stem Cells to Model Disease.** *Cell Stem Cell* 2009, **5**(6):584-595.
31. Martino F, Perestrelo AR, Vinarský V, Pagliari S, Forte G: **Cellular Mechanotransduction: From Tension to Function.** *Frontiers in Physiology* 2018, **9**(824).
32. Reilly GC, Engler AJ: **Intrinsic extracellular matrix properties regulate stem cell differentiation.** *Journal of Biomechanics* 2010, **43**(1):55-62.
33. Panciera T, Azzolin L, Cordenonsi M, Piccolo S: **Mechanobiology of YAP and TAZ in physiology and disease.** *Nature Reviews Molecular Cell Biology* 2017, **18**:758.
34. McCarty WJ, Usta OB, Yarmush ML: **A Microfabricated Platform for Generating Physiologically-Relevant Hepatocyte Zonation.** *Scientific Reports* 2016, **6**:26868.
35. Beckwitt CH, Clark AM, Wheeler S, Taylor DL, Stolz DB, Griffith L, Wells A: **Liver ‘organ on a chip’.** *Experimental Cell Research* 2018, **363**(1):15-25.
36. Swinney DC, Anthony J: **How were new medicines discovered?** *Nat Rev Drug Discov* 2011, **10**(7):507-519.
37. Imming P, Sinning C, Meyer A: **Drugs, their targets and the nature and number of drug targets.** *Nat Rev Drug Discov* 2006, **5**(10):821-834.
38. Overington JP, Al-Lazikani B, Hopkins AL: **How many drug targets are there?** *Nat Rev Drug Discov* 2006, **5**(12):993-996.
39. Arrowsmith CH, Audia JE, Austin C, Baell J, Bennett J, Blagg J, Bountra C, Brennan PE, Brown PJ, Bunnage ME *et al*: **The promise and peril of chemical probes.** *Nat Chem Biol* 2015, **11**(8):536-541.
40. Kosaka T, Okuyama R, Sun W, Ogata T, Harada J, Araki K, Izumi M, Yoshida T, Okuno A, Fujiwara T *et al*: **Identification of Molecular Target of AMP-activated Protein Kinase Activator by Affinity Purification and Mass Spectrometry.** *Analytical Chemistry* 2005, **77**(7):2050-2055.
41. King FJ, Selinger DW, Mapa FA, Janes J, Wu H, Smith TR, Wang Q-Y, Niyomrattanakitand P, Sipes DG, Brinker A *et al*: **Pathway Reporter Assays Reveal Small Molecule Mechanisms of Action.** *Journal of the Association for Laboratory Automation* 2009, **14**(6):374-382.
42. Michael S, Auld D, Klumpp C, Jadhav A, Zheng W, Thorne N, Austin CP, Inglese J, Simeonov A: **A Robotic Platform for Quantitative High-Throughput Screening.** *ASSAY and Drug Development Technologies* 2008, **6**(5):637-657.
43. Rodier F, Campisi J: **Four faces of cellular senescence.** *The Journal of Cell Biology* 2011, **192**(4):547-556.

44. Giorgio M, Trinei M, Migliaccio E, Pelicci PG: **Hydrogen peroxide: a metabolic by-product or a common mediator of ageing signals?** *Nat Rev Mol Cell Biol* 2007, **8**(9):722-728.
45. Sayers CM, Papandreou I, Guttman DM, Maas NL, Diehl JA, Witze ES, Koong AC, Koumenis C: **Identification and Characterization of a Potent Activator of p53-Independent Cellular Senescence via a Small-Molecule Screen for Modifiers of the Integrated Stress Response.** *Molecular Pharmacology* 2013, **83**(3):594-604.
46. Campisi J: **Cellular senescence as a tumor-suppressor mechanism.** *Trends in Cell Biology* 2001, **11**(11):S27-S31.
47. McHugh Sutkowski E, Tang W-J, Broome CW, Robbins JD, Seamon KB: **Regulation of forskolin interactions with type I, II, V, and VI adenylyl cyclases by Gs.alpha.** *Biochemistry* 1994, **33**(43):12852-12859.
48. Cusack NJ, Hourani SM: **5'-N-ethylcarboxamidoadenosine: a potent inhibitor of human platelet aggregation.** *British Journal of Pharmacology* 1981, **72**(3):443-447.
49. Castagna M, Takai Y, Kaibuchi K, Sano K, Kikkawa U, Nishizuka Y: **Direct activation of calcium-activated, phospholipid-dependent protein kinase by tumor-promoting phorbol esters.** *Journal of Biological Chemistry* 1982, **257**(13):7847-7851.
50. Middleton JP, Khan WA, Collinsworth G, Hannun YA, Medford RM: **Heterogeneity of protein kinase C-mediated rapid regulation of Na/K-ATPase in kidney epithelial cells.** *Journal of Biological Chemistry* 1993, **268**(21):15958-15964.
51. Gustafson KR, Cardellina JH, McMahon JB, Gulakowski RJ, Ishitoya J, Szallasi Z, Lewin NE, Blumberg PM, Weislow OS: **A nonpromoting phorbol from the Samoan medicinal plant Homalanthus nutans inhibits cell killing by HIV-1.** *Journal of Medicinal Chemistry* 1992, **35**(11):1978-1986.
52. Ryves WJ, Evans AT, Olivier AR, Parker PJ, Evans FJ: **Activation of the PKC-isotypes  $\alpha$ ,  $\beta$ 1,  $\gamma$ ,  $\delta$ , and  $\epsilon$  by phorbol esters of different biological activities.** *FEBS Letters* 1991, **288**(1):5-9.
53. Zhu W-H, Majluf-Cruz A, Omburo GA: **Cyclic AMP-specific phosphodiesterase inhibitor rolipram and RO-20-1724 promoted apoptosis in HL60 promyelocytic leukemic cells via cyclic AMP-independent mechanism.** *Life Sciences* 1998, **63**(4):265-274.
54. Aoki M, Kobayashi M, Ishikawa J, Saita Y, Terai Y, Takayama K, Miyata K, Yamada T: **A Novel Phosphodiesterase Type 4 Inhibitor, YM976 (4-(3-Chlorophenyl)-1,7-diethylpyrido[2,3-d]pyrimidin-2(1H)-one), with Little Emetogenic Activity.** *Journal of Pharmacology and Experimental Therapeutics* 2000, **295**(1):255-260.
55. Whitaker RM, Wills LP, Stallons LJ, Schnellmann RG: **cGMP-Selective Phosphodiesterase Inhibitors Stimulate Mitochondrial Biogenesis and Promote Recovery from Acute Kidney Injury.** *The Journal of Pharmacology and Experimental Therapeutics* 2013, **347**(3):626-634.
56. Schudt C, Winder S, Müller B, Ukena D: **Zardaverine as a selective inhibitor of**

- phosphodiesterase isozymes.** *Biochemical Pharmacology* 1991, **42**(1):153-162.
57. Foulkes WD, Smith IE, Reis-Filho JS: **Triple-Negative Breast Cancer.** *New England Journal of Medicine* 2010, **363**(20):1938-1948.
  58. Chavez KJ, Garimella SV, Lipkowitz S: **Triple Negative Breast Cancer Cell Lines: One Tool in the Search for Better Treatment of Triple Negative Breast Cancer.** *Breast Disease* 2010, **32**(1-2):35-48.
  59. Terao Y, Nishida J-i, Horiuchi S, Rong F, Ueoka Y, Matsuda T, Kato H, Furugen Y, Yoshida K, Kato K *et al*: **Sodium butyrate induces growth arrest and senescence-like phenotypes in gynecologic cancer cells.** *International Journal of Cancer* 2001, **94**(2):257-267.
  60. Clevers H, Nusse R: **Wnt/ $\beta$ -Catenin Signaling and Disease.** *Cell* 2012, **149**(6):1192-1205.
  61. Liu J, Wu X, Mitchell B, Kintner C, Ding S, Schultz PG: **A Small-Molecule Agonist of the Wnt Signaling Pathway.** *Angewandte Chemie International Edition* 2005, **44**(13):1987-1990.
  62. Coghlan MP, Culbert AA, Cross DAE, Corcoran SL, Yates JW, Pearce NJ, Rausch OL, Murphy GJ, Carter PS, Roxbee Cox L *et al*: **Selective small molecule inhibitors of glycogen synthase kinase-3 modulate glycogen metabolism and gene transcription.** *Chemistry & Biology* 2000, **7**(10):793-803.
  63. Cupido T, Rack PG, Firestone AJ, Hyman JM, Han K, Sinha S, Ocasio CA, Chen JK: **The Imidazopyridine Derivative JK184 Reveals Dual Roles for Microtubules in Hedgehog Signaling.** *Angewandte Chemie International Edition* 2009, **48**(13):2321-2324.
  64. Dumontet C, Jordan MA: **Microtubule-binding agents: a dynamic field of cancer therapeutics.** *Nat Rev Drug Discov* 2010, **9**(10):790-803.
  65. Mahboobi S, Pongratz H, Hufsky H, Hockemeyer J, Frieser M, Lyssenko A, Paper DH, Bürgermeister J, Böhmer F-D, Fiebig H-H *et al*: **Synthetic 2-Aroylindole Derivatives as a New Class of Potent Tubulin-Inhibitory, Antimitotic Agents.** *Journal of Medicinal Chemistry* 2001, **44**(26):4535-4553.
  66. Bonne D, Heuséle C, Simon C, Pantaloni D: **4',6-Diamidino-2-phenylindole, a fluorescent probe for tubulin and microtubules.** *Journal of Biological Chemistry* 1985, **260**(5):2819-2825.
  67. Jordan MA, Thrower D, Wilson L: **Effects of vinblastine, podophyllotoxin and nocodazole on mitotic spindles. Implications for the role of microtubule dynamics in mitosis.** *Journal of Cell Science* 1992, **102**(3):401-416.
  68. Gewirtz DA, Holt SE, Elmore LW: **Accelerated senescence: An emerging role in tumor cell response to chemotherapy and radiation.** *Biochemical Pharmacology* 2008, **76**(8):947-957.
  69. Tierno MB, Kitchens CA, Petrik B, Graham TH, Wipf P, Xu FL, Saunders WS, Raccor BS, Balachandran R, Day BW *et al*: **Microtubule Binding and Disruption and Induction of Premature Senescence by Disorazole C1.** *Journal of Pharmacology and Experimental Therapeutics* 2009, **328**(3):715-722.

70. Croft D, Mundo AF, Haw R, Milacic M, Weiser J, Wu G, Caudy M, Garapati P, Gillespie M, Kamdar MR *et al*: **The Reactome pathway knowledgebase**. *Nucleic Acids Research* 2014, **42**(Database issue):D472-D477.
71. Bunnage ME, Chekler ELP, Jones LH: **Target validation using chemical probes**. *Nature Chemical Biology* 2013, **9**:195.
72. Katayama R, Aoyama A, Yamori T, Qi J, Oh-hara T, Song Y, Engelman JA, Fujita N: **Cytotoxic Activity of Tivantinib (ARQ 197) Is Not Due Solely to c-MET Inhibition**. *Cancer Research* 2013, **73**(10):3087-3096.
73. Martin YC, Kofron JL, Traphagen LM: **Do Structurally Similar Molecules Have Similar Biological Activity?** *Journal of Medicinal Chemistry* 2002, **45**(19):4350-4358.
74. Mohan R, Banerjee M, Ray A, Manna T, Wilson L, Owa T, Bhattacharyya B, Panda D: **Antimitotic Sulfonamides Inhibit Microtubule Assembly Dynamics and Cancer Cell Proliferation**. *Biochemistry* 2006, **45**(17):5440-5449.
75. Wang Y, Debatin K-M, Hug H: **HIPK2 overexpression leads to stabilization of p53 protein and increased p53 transcriptional activity by decreasing Mdm2 protein levels**. *BMC Molecular Biology* 2001, **2**:8-8.
76. Lukas J, Herzinger T, Hansen K, Moroni MC, Resnitzky D, Helin K, Reed SI, Bartek J: **Cyclin E-induced S phase without activation of the pRb/E2F pathway**. *Genes & Development* 1997, **11**(11):1479-1492.
77. Wang Y, Shen J, Arenzana N, Tirasophon W, Kaufman RJ, Prywes R: **Activation of ATF6 and an ATF6 DNA Binding Site by the Endoplasmic Reticulum Stress Response**. *Journal of Biological Chemistry* 2000, **275**(35):27013-27020.
78. Kinzler KW, Vogelstein B: **The GLI gene encodes a nuclear protein which binds specific sequences in the human genome**. *Molecular and Cellular Biology* 1990, **10**(2):634-642.
79. Huang LE, Arany Z, Livingston DM, Bunn HF: **Activation of Hypoxia-inducible Transcription Factor Depends Primarily upon Redox-sensitive Stabilization of Its  $\alpha$  Subunit**. *Journal of Biological Chemistry* 1996, **271**(50):32253-32259.
80. Piek E, Westermark U, Kastemar M, Heldin C-H, van Zoelen EJ, Nistér M, Ten Dijke P: **Expression of transforming-growth-factor (TGF)- $\beta$  receptors and Smad proteins in glioblastoma cell lines with distinct responses to TGF- $\beta$ 1**. *International Journal of Cancer* 1999, **80**(5):756-763.
81. Molenaar M, van de Wetering M, Oosterwegel M, Peterson-Maduro J, Godsave S, Korinek V, Roose J, Destree O, Clevers H: **XTcf-3 Transcription Factor Mediates  $\beta$ -Catenin-Induced Axis Formation in Xenopus Embryos**. *Cell* 1996, **86**(3):391-399.
82. Yang XO, Pappu B, Nurieva R, Akimzhanov A, Kang HS, Chung Y, Ma L, Shah B, Panopoulos AD, Schluns K *et al*: **TH17 lineage differentiation is programmed by orphan nuclear**

- receptors ROR $\alpha$  and ROR $\gamma$ . *Immunity* 2008, **28**(1):29-39.
83. Choudhury D, Ahmed Z: **Drug-associated renal dysfunction and injury**. *Nat Clin Pract Neph* 2006, **2**(2):80-91.
84. Ozkok A, Edelstein CL: **Pathophysiology of Cisplatin-Induced Acute Kidney Injury**. *BioMed Research International* 2014, **2014**:17.
85. Shah SR, Tunio SA, Arshad MH, Moazzam Z, Noorani K, Feroze AM, Shafquat M, Hussain HS, Jeoffrey SAH: **Acute Kidney Injury Recognition and Management: A Review of the Literature and Current Evidence**. *Global Journal of Health Science* 2016, **8**(5):120-124.
86. Tiong HY, Huang P, Xiong S, Li Y, Vathsala A, Zink D: **Drug-Induced Nephrotoxicity: Clinical Impact and Preclinical in Vitro Models**. *Molecular Pharmaceutics* 2014, **11**(7):1933-1948.
87. Wang L, Sweet DH: **Renal Organic Anion Transporters (SLC22 Family): Expression, Regulation, Roles in Toxicity, and Impact on Injury and Disease**. *The AAPS Journal* 2013, **15**(1):53-69.
88. Masereeuw R, Russel FGM: **Regulatory Pathways for ATP-binding Cassette Transport Proteins in Kidney Proximal Tubules**. *The AAPS Journal* 2012, **14**(4):883-894.
89. Yonezawa A, Inui K-i: **Importance of the multidrug and toxin extrusion MATE/SLC47A family to pharmacokinetics, pharmacodynamics/toxicodynamics and pharmacogenomics**. *British Journal of Pharmacology* 2011, **164**(7):1817-1825.
90. Jenkinson SE, Chung GW, van Loon E, Bakar NS, Dalzell AM, Brown CDA: **The limitations of renal epithelial cell line HK-2 as a model of drug transporter expression and function in the proximal tubule**. *Pflügers Archiv - European Journal of Physiology* 2012, **464**(6):601-611.
91. Frohlich EM, Zhang X, Charest JL: **The use of controlled surface topography and flow-induced shear stress to influence renal epithelial cell function**. *Integrative Biology* 2012, **4**(1):75-83.
92. Jang K-J, Mehr AP, Hamilton GA, McPartlin LA, Chung S, Suh K-Y, Ingber DE: **Human kidney proximal tubule-on-a-chip for drug transport and nephrotoxicity assessment**. *Integrative Biology* 2013, **5**(9):1119-1129.
93. Yasujima T, Ohta K-y, Inoue K, Ishimaru M, Yuasa H: **Evaluation of 4',6-Diamidino-2-phenylindole as a Fluorescent Probe Substrate for Rapid Assays of the Functionality of Human Multidrug and Toxin Extrusion Proteins**. *Drug Metabolism and Disposition* 2010, **38**(4):715-721.
94. Langfelder P, Horvath S: **WGCNA: an R package for weighted correlation network analysis**. *BMC Bioinformatics* 2008, **9**(1):1-13.
95. Tian Y, Voineagu I, Paşca SP, Won H, Chandran V, Horvath S, Dolmetsch RE, Geschwind DH: **Alteration in basal and depolarization induced transcriptional network in iPSC derived**

- neurons from Timothy syndrome.** *Genome Medicine* 2014, **6**(10):1-16.
96. Ito S, Kusuhara H, Kuroiwa Y, Wu C, Moriyama Y, Inoue K, Kondo T, Yuasa H, Nakayama H, Horita S *et al*: **Potent and Specific Inhibition of mMate1-Mediated Efflux of Type I Organic Cations in the Liver and Kidney by Pyrimethamine.** *Journal of Pharmacology and Experimental Therapeutics* 2010, **333**(1):341-350.
97. Liby K, Hock T, Yore MM, Suh N, Place AE, Risingsong R, Williams CR, Royce DB, Honda T, Honda Y *et al*: **The Synthetic Triterpenoids, CDDO and CDDO-Imidazolide, Are Potent Inducers of Heme Oxygenase-1 and Nrf2/ARE Signaling.** *Cancer Research* 2005, **65**(11):4789-4798.
98. Hur W, Sun Z, Jiang T, Mason DE, Peters EC, Zhang DD, Luesch H, Schultz PG, Gray NS: **A Small-Molecule Inducer of the Antioxidant Response Element.** *Chemistry & Biology* 2010, **17**(5):537-547.
99. Yuan X, Xu C, Pan Z, Keum Y-S, Kim J-H, Shen G, Yu S, Oo KT, Ma J, Kong A-NT: **Butylated hydroxyanisole regulates ARE-mediated gene expression via Nrf2 coupled with ERK and JNK signaling pathway in HepG2 cells.** *Molecular Carcinogenesis* 2006, **45**(11):841-850.
100. Vollrath V, Wielandt Ana M, Iruretagoyena M, Chianale J: **Role of Nrf2 in the regulation of the Mrp2 (ABCC2) gene.** *Biochemical Journal* 2006, **395**(Pt 3):599-609.
101. Ashino T, Yamamoto M, Numazawa S: **Nrf2/Keap1 system regulates vascular smooth muscle cell apoptosis for vascular homeostasis: role in neointimal formation after vascular injury.** *Scientific Reports* 2016, **6**:26291.
102. Duncombe TA, Tentori AM, Herr AE: **Microfluidics: reframing biological enquiry.** *Nature Reviews: Molecular Cell Biology* 2015, **16**(9):554-567.
103. Esch EW, Bahinski A, Huh D: **Organs-on-chips at the frontiers of drug discovery.** *Nature Reviews: Drug Discovery* 2015, **14**(4):248-260.
104. Kansanen E, Kuosmanen SM, Leinonen H, Levonen A-L: **The Keap1-Nrf2 pathway: Mechanisms of activation and dysregulation in cancer.** *Redox Biology* 2013, **1**(1):45-49.
105. Ali F, Zakkar M, Karu K, Lidington EA, Hamdulay SS, Boyle JJ, Zloh M, Bauer A, Haskard DO, Evans PC *et al*: **Induction of the Cytoprotective Enzyme Heme Oxygenase-1 by Statins Is Enhanced in Vascular Endothelium Exposed to Laminar Shear Stress and Impaired by Disturbed Flow.** *Journal of Biological Chemistry* 2009, **284**(28):18882-18892.
106. Bryan MT, Duckles H, Feng S, Hsiao ST, Kim HR, Serbanovic-Canic J, Evans PC: **Mechanoresponsive Networks Controlling Vascular Inflammation.** *Arteriosclerosis, Thrombosis, and Vascular Biology* 2014, **34**(10):2199-2205.
107. Hsieh C-Y, Hsiao H-Y, Wu W-Y, Liu C-A, Tsai Y-C, Chao Y-J, Wang DL, Hsieh H-J: **Regulation of shear-induced nuclear translocation of the Nrf2 transcription factor in**

- endothelial cells.** *Journal of Biomedical Science* 2009, **16**(1):12-12.
108. Wang X, Campos CR, Peart JC, Smith LK, Boni JL, Cannon RE, Miller DS: **Nrf2 Upregulates ATP Binding Cassette Transporter Expression and Activity at the Blood–Brain and Blood–Spinal Cord Barriers.** *The Journal of Neuroscience* 2014, **34**(25):8585-8593.
109. Shin S, Wakabayashi N, Misra V, Biswal S, Lee GH, Agoston ES, Yamamoto M, Kensler TW: **NRF2 Modulates Aryl Hydrocarbon Receptor Signaling: Influence on Adipogenesis.** *Molecular and Cellular Biology* 2007, **27**(20):7188-7197.
110. Wu KC, Cui JY, Klaassen CD: **Effect of Graded Nrf2 Activation on Phase-I and -II Drug Metabolizing Enzymes and Transporters in Mouse Liver.** *PLoS One* 2012, **7**(7):e39006.
111. Martovetsky G, Tee JB, Nigam SK: **Hepatocyte Nuclear Factors 4 $\alpha$  and 1 $\alpha$  Regulate Kidney Developmental Expression of Drug-Metabolizing Enzymes and Drug Transporters.** *Molecular Pharmacology* 2013, **84**(6):808-823.
112. Ogasawara K, Terada T, Asaka J-i, Katsura T, Inui K-i: **Hepatocyte nuclear factor-4 $\alpha$  regulates the human organic anion transporter 1 gene in the kidney.** *American Journal of Physiology - Renal Physiology* 2007, **292**(6):F1819-F1826.
113. Desai SS, Tung JC, Zhou VX, Grenert JP, Malato Y, Rezvani M, Español-Suñer R, Willenbring H, Weaver VM, Chang TT: **Physiological ranges of matrix rigidity modulate primary mouse hepatocyte function in part through hepatocyte nuclear factor 4 alpha.** *Hepatology* 2016, **64**(1):261-275.